IMPACTS OF ENERGY STORAGE AND SMART RESTORATION ON THE RELIABILITY OF ELECTRIC MICROGRID

BY

NEMER ABD ALHALIM MOHAMMAD AMLEH

A Thesis Presented to the

DEANSHIP OF GRADUATE STUDIES

KING FAHD UNIVERSITY OF PETROLEUM & MINERALS

DHAHRAN, SAUDI ARABIA

In Partial Fulfillment of the

Requirements for the Degree of

MASTER OF SCIENCE

In

ELECTRICAL ENGINEERING

MAY 2016

KING FAHD UNIVERSITY OF PETROLEUM & MINERALS

DHAHRAN- 31261, SAUDI ARABIA

DEANSHIP OF GRADUATE STUDIES

This thesis, written by **NEMER ABD AL HALIM MOHAMMAD AMLEH** under the direction his thesis advisor and approved by his thesis committee, has been presented and accepted by the Dean of Graduate Studies, in partial fulfillment of the requirements for the degree of **MASTER OF SCIENCE IN ELECTRICAL ENGINEERING.**

muhaini

Dr. Mohammad Al-Muhaini
(Advisor)

Dr. Ali A. Al-Shaikhi

Department Chairman

Prof. Ibrahim El Amin

(Member)

Prof. Salam A. Zummo
Dean of Graduate Studies

Ali Al-Awami

Dr. Ali T. Al Awami

(Member)

3/5/16

Date

Dedication

To my father for his love, prayers and tender, God bless his soul. To my merciful mother for her love, prayers and support. To my dear brothers and sisters for their love, help and encouragement. To all my family members for their love and good wishes.

ACKNOWLEDGMENTS

In the name of Allah

The praise and thank to Allah, who guided and helped me in completing this work. Thanks to King Fahd University of Petroleum and Minerals, which is one of the top universities in Arabic world.

I would like to introduce my sincere gratitude and profound thanks to my advisor, Dr. Mohammad M. Al Muhaini, for his intellectual support and invaluable advice and assistance during my study and throughout achieving this work.

Thanks to my thesis committee members, Prof. Ibrahim El Amin and Dr. Ali Al Awami, for their constructive comments and guidance. Thanks to my teachers for their help during my study. Thanks to my friends for their advising and untangible support.

Last but not least, special thanks to all my family, especially my beloved mother, brothers and sisters, who have been an important and indispensible source of motivation and inspiration.

TABLE OF CONTENTS

LIST OF TABLES

LIST OF FIGURES

NOMENCLATURE

$\boldsymbol{\alpha}$	:	Smoothing constant
$\boldsymbol{\alpha_i}$	:	Coefficients of AR terms
ARMA	:	Autoregressive moving average
ARIMA	:	Autoregressive integrated moving average
$\boldsymbol{\beta_i}$	:	Coefficients of MA terms
$\boldsymbol{D_t}$	:	Demand at hour t
DER	:	Distribution energy resources
DG	:	Distributed generation
$\boldsymbol{e}(\boldsymbol{t})$	:	White Gaussian noise with zero mean
$\boldsymbol{Ec_t}$	:	Energy for charge at hour t
$\boldsymbol{Ed_t}$	:	Energy for discharge at hour t
ENS	:	Energy not supplied
EENS	:	Expected energy not supplied
EENU	:	Expected energy not used
ES	:	Energy storage
ESS	:	Energy storage system
EV	:	Electrical vehicle

$\boldsymbol{F_t}$	:	Previous forecasted of current period
$\boldsymbol{F_{t+1}}$	:	Forecasted value of future period
$\boldsymbol{\lambda}$	:	Failure rate (f/y)
LP	:	Load point
MCS	:	Monte Carlo simulation
MG	:	Microgrid
MTTF	:	Mean time between failurs
MTTR	:	Mean time between repairs
N	:	Sample size
$\boldsymbol{\mu}$	:	Repair rate
P	:	Number of AR terms
$\boldsymbol{P_r}$	:	Rated power of wind turbine generator (WTG)
$\boldsymbol{P_t}$	:	Actual value of PV output
$\boldsymbol{P(WS_t)}$	:	Output power of WTG
PV	:	Photovoltaic
Q	:	Number of MA terms
$\boldsymbol{R_c}$	:	Charging rate
$\boldsymbol{R_d}$	:	Discharging rate

RBTS	:	Roy Billinton test system
RE	:	Renewable energy
RES	:	Renewable energy source
SAIDI	:	System average interruption duration index
SAIFI	:	System average interruption frequency index
$\boldsymbol{\sigma^2}$	:	Wind speed error variance
$\boldsymbol{SOC(t)}$	:	Battery state of charge at hour t
$\boldsymbol{SOC^{max}}$	:	Max Battery state of charge
$\boldsymbol{SOC^{min}}$	:	Min Battery state of charge
SP	:	Solar power
UPS	:	Uninterruptable power supply
$\boldsymbol{V_{ci}}$	:	Cut in speed
$\boldsymbol{V_{co}}$	:	Cut out speed
$\boldsymbol{V_r}$	:	Rated speed
WP	:	Wind power
WS	:	Wind speed
$\boldsymbol{WS_t}$	:	Wind speed at hour t
WT	:	Wind turbine

WTG	:	Wind turbine generator
$\boldsymbol{X(t)}$	:	Time series data

ABSTRACT

Full Name	:	Nemer Abd Al Halim Mohammad Amleh
Thesis Title	:	Impacts of Eenrgy Storage and Smart Restoration on the Reliability of Electric Microgrid
Major Field	:	Electrical Engineering
Date of Degree	:	May 2016

The development and utilization of renewable energy sources (RES), especially wind and solar, has been given important consideration due to the increased consumption of conventional energy resources and enhanced public awareness of the potential impact of conventional energy systems on the environment. However, RES have a random and intermittent nature that affects their reliability in electrical networks.

In the 21st century, the concept of smart grid, which began and formed gradually, has become a promising choice to face future challenges. Self-healing is an important feature of the smart grid. The main task of self-healing control is real-time monitoring of network operation, predicting the state of the power grid, timely detection, rapid diagnosis, and elimination of hidden faults, without human intervention.

The main aim of the thesis is to study the reliability of islanded microgrids under the utilization of smart restoration and ESS to assess the acquired improvements in power grid reliability. Therefore, this thesis implements smart restoration and energy storage units to increase the reliability of a stand-alone microgrid (MG) system. The wind and solar energy resources are considered to be the main energy resources in MG. Two

models are implemented to reduce the effects of uncertainty in the wind- and solar-generated power, the ARMA model for wind speed and the triple exponential smoothing model for solar energy prediction. The study was carried out on Roy Billinton test system (RBTS).

ملخص الرسالة

الاسم الكامل : نمر عبدالحليم محمد عملة

عنوان الرسالة : آثار تخزين الطاقة الكهربائية وإستعادة التغذية الذكية على موثوقية شبكة الكهرباء الصغيرة

التخصص : الهندسة الكهربائية

تاريخ الدرجة العلمية : رجب 1437

التطور والاستفادة من مصادر الطاقة المتجددة - خصوصا الرياح والشمس - بات أمرا واضحا يعطى اعتبارا هاما بسبب ما يتعلق بالاستهلاك المتزايد لموارد الوقود الاحفوري و زيادة الوعي العام حول الآثار السيئة لهذه الموارد على البيئة. ولكن مصادر الطاقة المتجددة أيضا لها سلبيات في أنها تمتلك طبيعة متقطعة وعشوائية التي تؤثر سلبا في موثوقية شبكات الكهرباء.

في القرن 21 ظهر مفهوم الشبكات الذكية و تشكل تدريجيا ليصبح خيارا مشتركا في موجهة التحديات المستقبلية. نظام اعادة التشغيل الذكي هو يعتبر من أهم مكونات هذه الشبكات. أهم مهمات هذا النظام هو المراقبة المستمرة لعمل الشبكة، التنبّأ بحالة الشبكة، التشخيص السريع للأعطال وإزالتها دون تدخل العنصر البشري.

هدف هذه الرسالة الرئيسي هو الاستقصاء البحثي لموثوقيّة الشبكات الصغيرة المعزولة في ظل وجود نظام الاستعادة الذكي و وحدات تخزين الطاقة الكهربائية لمعرفة مدى المنافع المحصّلة على الموثوقيّة من استخدام هذا النظام. لذلك هذه الرسالة تستعمل هذا النظام ووحدات تخزين الطاقة لزيادة موثوقية الشبكات الصغيرة المعزولة عن الشبكة الرئيسية التي تستعل الرياح والشمس كمصدر أساسي. بحثت هذه الرسالة نموذجين للتنبؤ بسرعة الرياح و الطاقة الشمسية وذلك للتقليل من أثر اللايقينية في القدرة الكهربائية المولدة من هذه المصادر. هذين النموذجين هما نموذج آرما الذي استخدم في تقدير سرعة الرياح و نموذج التحسين الاسي لتقدير القدرة الكهربائية المولدة من الطاقة الشمسية. ولتحقيق أهداف هذه الرسالة، فقد اجريت هذه الدراسة على شبكة صغيرة ممثلة بنموذج روي بلنتون التوزيعي لأغراض دراسة و تحليل موثوقية شبكات التوزيع المعزولة.

Chapter 1

INTRODUCTION

1.1. Overview

Sun and wind are considered as green sources because of their negligible contribution in greenhouse gas emissions. These sources have been considered as an alternative energy to fossil fuels since the 1970s [1]. However, renewable energy remained inactive until the 2000s because of its high energy production costs during that period [2]. During 2000s, the use of renewable energy increased due to the advancement in their technologies. For example, the generated solar photovoltaic (PV) energy reached 102 GW in 2012 while wind energy reached 282 GW [3].

During 2000s, the technological advancements in renewable energy generation has allowed the use of the telecommunication technology in the power systems, which is known the smart grid. Its main function is to continuously monitor, detect, and diagnose any change in the network. It is able to change the network topology and deal with the bidirectional power flow. One of the most important features of the smart grid is the smart restoration as the system. The smart restoration is an integrated system of telecommunication equipment and computer devices to locate and restore the interrupted loads based on their priorities. One of the most important characteristics in the smart restoration is its ability in optimizing the switch operations sequence. Thus, it optimizes the grid's operation and reliability. Moreover, it can operate the distributed generation

(DG) resources and associated ESS units efficiently and strategically taking into account the different technical and environmental issues.

An important feature in the smart grid is its ability in employing the demand side management (DSM). It can control the demand and allow the demand response schemes easily through the smart meters and sensors. The smart grid can improve the reliability and allow a large deployment of the renewable energy sources (RES). However, using of smart restoration only cannot completely solve the random intermittency of the renewable energy. Controlling demand option could be suggested as solution for the aforementioned problem. Nonetheless, with existence of fluctuating and intermittent energy sources, flexible demand has shown little ability [4].

The remaining option in which these fluctuations can be suppressed efficiently is by using an ESS, as several studies proved this claim [5]-[7]. The recent developments in energy storage and power electronics have increased the energy storage applications in the modern power systems. These advancements made the ESS as the best solution for intermittency of renewable energy. Therefore, smart restoration and energy storage facilitate the integration of renewable resources, improve system reliability and enhance the efficiency of transmission and distribution networks.

1.2. Thesis Motivations

The increased focus on renewable energy motivates studies concerning the renewable energy integration into existing energy supply systems. Wind energy and solar energy are expected to play a key role in the future energy supply. Using of these sources is very important to reduce the impact of the emissions of greenhouse gases (CO2, NOx, SOx). Nevertheless, the electricity generation from wind and sun is always fluctuating due to their intermittent nature that depends on the environmental status. Moreover, forecasting solar and wind power involves uncertainties. In islanded systems, MG reliability and power availability became a main concern.

The use of secondary dispatchable generators is a good option that can be used to reduce power intermittency impacts. A second option is storing the generated energy at times of low-demand so as to be released at times of high-demand. Although energy storage can solve the power intermittency or uncertainty effects, but it cannot well overcome the power lines or units outages at large scale.

The best option that can be used to enhance the reliability of microgrid system in islanded case is the use of smart restoration. The smart restoration can overcome the interruptions and outages through finding another route and coordinating the supply with demand. It can diminish the interrupted area and optimize the usage of the energy resources. However, matching the energy generation from renewable resources with the load to satisfy the balance condition is problematic. Implementing the smart restoration to improve the reliability of stand-alone microgrids is a challenging issue and the thesis attempts to investigate this issue using Monte Carlo simulation (MCS).

1.3. Thesis Objectives

The main objective of this thesis is studying and implementing the smart restoration theoretically to improve the stand-alone microgrid reliability. The objectives of this thesis are summarized as follow:

1) Modeling and simulation of the short-term wind speed and solar power.

2) Evaluating the reliability of stand-alone microgrid system when the renewable energy and energy storage are the main energy supply system in microgrid, and including the uncertainty in the renewable energy.

3) Investigating the capability of the smart restoration in improving the reliability of stand-alone microgrid system.

1.4. Thesis Outline

This thesis is organized as follows:

Chapter 2 provides background about microgrids concept, reliability of the microgrids as well as self healing of the microgrids. In addition, it includes background about renewable energy sources and energy storage. This chapter also includes an overall literature review on current approaches for self-healing of microgrids and their reliability. It also includes literature review on renewable energy-based DG integration and energy storage usage in distribution networks. Chapter 3 describes the system modeling of the wind speed, solar power, load modeling, energy storage and their reliability models. It introduces background on Monte Carlo simulation (MCS) and the smart restoration impact on the reliability of the microgrid.

Chapter 4 presents case studies on the positive impacts of using of the smart restoration and the energy storage on the reliability of the microgrid. It also includes case studies on the effects of the power capacity and the uncertainties in the generated power from the wind and sun. Finally, Chapter 5 concludes the research in this thesis. The directions for further research are also presented in this chapter.

Chapter 2

LITERATURE REVIEW

2.1 Microgrid

Microgrid is a low voltage distribution network that delivers the power to small communities [9]. The power can flow locally and the consumer can participate in the electricity enterprise. It combines different renewable energy resources with conventional substations such as diesel stations. As it acts either as a net load to main grid or a power supply (islanded operation). It contributes to reduce the carbon emission locally due to using the renewable energy, enable of using several energy resources and reducing cost [10]. In microgrid, a simultaneous group of generating units are operated together for the benefit of its members. The supply sources may include engine generator sets, micro turbines, fuel cells, photovoltaic, and other small-scale renewable generators [11].

These microgrids solve the problems associated with penetration of renewable energy-based distributed generators (DG) and make the bulk grid suitable for large scale deployment of DGs. They make the controlling of the DGs in more flexible way and reduce the centralized management of the system [12].

2.2 Reliability of Microgrid and Self-healing of the Power System

Reliability of microgrid studies the unavailability, number of incidents, no. of hours of interruption, no. of voltage violations that exceed the limits and no. of frequency excursions beyond the limits. In addition, reliability study of MG started to take into account the energy storage units that play a key role in minimizing the effects of renewable energy-based DGs and introduce a safe and stable operation of the MG. However, reliability of MG is more complicated because of using renewable-based DGs whose output power fluctuates, this leads to instability in the operation of the microgrid which in turn affects the reliability of the MG [13].

In addition, the reliability of the renewable energy resource is measured of how long the source generates a stable amount of energy. These resources generate electricity in an intermittent and unstable way and it can't rely on. Therefore, they are used in energy mix to introduce a flexible back up generation [14]. On the other hand, dispatchable energy resource is considered reliable if it can generate the required electrical energy to meet the demand.

Accordingly, reliability analysis of MG should take into account the natural characteristics of these resources. i.e., wind is characterized as an intermittent and unstable source because wind speed has time-varying nature and not constant, which may not supply the peak demand when needed. However, reliability of wind power system can be increased by using the power electronics and programmable controller to allow a flexible controlling of the wind turbine [15]. Solar energy also is considered as an intermittent source because it depends on the geographical area and it does not shine at night. On the other hand, like wind power system, availability of solar power can be increased by the usage of energy storage system (ESS). While Hydro-electrical power is considered reliable because it can generates the electricity as long as there is a plenty of water flows into turbines. Since we can control the amount of water to flow through the turbine, we can control the amount of electrical power to be supplied and thus the reliability is high [14].

The reliability evaluation methods in MG are basically two, frequency and duration method and Monte Carlo simulation (MCS) method that can be used to determine the MG's contribution to reliability of bulk grid and the MG itself [16]. In [17], an assessment of the benefits of MG on reliability of power system has been proposed using MCS and applied to the IEEE-RBTS system. It has shown that MGs significantly enhance the reliability of the bulk grid.

Ref. [9] proposed evaluation method of Availability of MG using MCS during natural disasters. It addressed the effects of life lines performance and local energy storage on the MG availability during natural disasters. The study disclosed that MG achieves much more availability than the bulk grid in these circumstances. Another study showed that MG improved reliability and decreased SAIFI and SAIDI by incorporating DER with variable capacity [19].

Self-healing is the self-restoring of the power grid to its normal operation using advanced monitoring methods that continuously diagnose and assess the operational status of the grid and remove any fault without affecting the supplied load [20]. The problem of self-healing consists of finding the sequence of switch operations that optimize the restoration state [21]. Its main functions are to evaluate the power grid behavior in a real time manner and help the grid to response quickly to any disturbance. And lastly, it isolates the disturbance and restores the grid to its normal state quickly [22].

Self-healing in the microgrid is more complicated than in the conventional networks due to the distribution network generators, distributed storage devices and electrical vehicles [21]. The difficulty of implementing the self-healing in the distribution network is also due to the new initial conditions that vary at each outage due to the mobile loads and existence of the renewable energy sources [21]. However, this can be improved by using the smart meters and sensors that increase the observability of the system and provide real time data about the status of the distributer line [23].

Self-healing nowadays is an important topic and many researches have been achieved and numerous works are now being done in this area. i.e., self-healing control structure has been accomplished in the smart distribution grid that consists of three layers [24]: Base layer which is the power grid and it should be able to accept the clean energy and deal with bidirectional power flow. Secondly, Support layer which is the data and communication equipment. Lastly, application layer which consists of monitoring, decision-making, assessment, Control and recovery to achieve self-healing of power grid. While self-healing structure depends on the intelligent agents has been proposed in [25]. This structure uses the intelligent agents and smart meters in order to estimate and control the load and restore the electricity grid. The passive and active networks, where automatic switches can be controlled via an agent, have been studied by this method. But it assumed that the operation process should be based on synchronized measurements. Another intelligent agents-based self-healing method that uses distributed energy storage has been proposed in [26]. This method uses the series and shunt agents to control the restoration process.

Self-healing methods in the distribution network are divided into local control, centralized and distributed self-healing [27]. Local control method uses relay devices to recover from fault and thus no need of communication. But it can only handle transient fault not to fix permanent fault. Centralized control relies on the main station to maintain the topology model. However, when the distribution network is complex, centralized self-healing takes longer time. On the other hand, distributed self-healing relies on smart pole switch to locate fault, isolate and restore power supply. Which makes its response faster. Accordingly, ref. [27] proposed the pole switches method to enhance the self-healing problems associated with local control self-healing strategy.

Other works reconfigured smart restoration based on tree-structured grid technique as in [28]. It showed that dividing bulk grid into islands improves power supply reliability and reduces size of the area of power outage. However, implementing this approach is difficult due to the problem of adjusting to a full agreement either in frequency, voltage or phase angle between two or more separate systems before integration [29]. Accordingly, the latter proposed a practical method and disclosed solid conclusions, can be dependent on, which mitigate the aforementioned problem. It showed that a reliable integration between MG and the bulk grid requires the voltage difference between them smaller enough while the frequency of the external grid should be slightly greater than the frequency of MG and the phase angle of the external grid should lead MG phase angle. Some works tried to improve reliability of MG by incorporating demand response (DR) scheme in self-healing [30]. It converted the reliability problem into an optimization problem that minimizes the total operation cost of energy not supplied (ENS) due to DR scheme. It used the load curtailment program to diminish the interrupted loads in MG. However, selecting a candidate load for restoring has major impact on final outage cost. It didn't consider the other option which is the increasing of generation in each MG by using new DGs.

Many studies researched self-healing in microgrid using the distributed self-healing i.e. ref. [31] studied service restoration (SR) in microgrid and introduced two sub-optimal solutions close to the optimal solution under the unscheduled disconnection from the main grid scenario. These solutions have been obtained based upon stochastic information. It argued that ESS plays a critical role in decreasing the negative impacts of the uncertainties of the forecasted renewable power generation. Other study in ref. [32] outlined the achievements towards realizing a smart microgrid at British Columbia Institute of Technology (BCIT) at Canada. It researched the design of the smart microgrid including protection and control scheme of the microgrid during the presence and absence of the utility connection. Ref. [33] has proposed a stable multiagents system (MAS)-based load restoration algorithm for microgrid. The study stated that the advantage of this method is that can be applied to power system of any size and configuration in addition to its guaranteed stability.

2.3 Renewable Energy and Energy Storage Applications

Renewable Energy (RE) is one of the best solutions to the depletion of energy resources and the environmental issues such as the global warming, CO_2 emission and others [34]. These nonconventional sources can be used in reducing the total electricity production cost. As it can be utilized in Micro-grids (MG) to suppress the expansion of the transmission grid to remote isolated areas. In addition, RE contributes in reducing the maintenance and transmission costs of the fuel of diesel generators that are commonly used in these places [35]. Recently, the world has witnessed increasing growth in RE sources (RES) especially in wind power, many countries are getting a considerable percentage of their electricity generation from RES. [34]. But due to most of RES are intermittent in its nature which increases power fluctuation and discontinuity in power supply limits its use and penetration in distribution networks.

On the other hand, the integration of an energy storage system (ESS) is one of the best solutions to ensure the power quality and stability of a power system with easing the penetration of RES such as wind energy. These energy storage (ES) devices introduce many services to the grid such as smoothing the power output from WTG, PV, etc. [36]-[39]. It contributes to system adequacy and improves power system reliability such as avoiding interruption of sensitive load and supply the load in uninterruptable power supply (UPS) fashion [40]. ES can be classified based on four parameters [34]; storage capacity, charging/discharging limit (max/min capacity of ES), charging/discharging efficiency and rated power of the energy storage unit. There are also other factors characterize ES, the operating strategies such as shaving of peak load, providing energy reserve, smoothing the output power from WTG [41] and priority of the RES [34].

2.3.1. Solar Power Modeling

One of the main challenges in the electrical grid is the integration of the solar power to the existing power supply systems. The main problem of integrating solar power into the existing electricity grid, lies in its discontinuous generation, because PV power drops when the solar irradiance decreases [42]. The fluctuations in PV power delivery to the grid cause problems for grid operators who must keep the balance between the generated power and the grid's load. Any implementation of the solar energy conversion process should take this behavior into account in its operating strategies. Hence, the short-term forecasting of the solar power is essential in optimizing the power system operations and increasing the participation of the solar power in the electricity grid. And the rising number of solar energy applications also increases the importance of the solar power forecast [43].

Several areas are affected by the short-term solar power forecasting such as: control, unit commitment, security assessment, optimum planning of power generation, energy exchange, grid integration. On the other hand, the solar power forecasting is affected by several factors such as: meteorological, climate, light intensity, dust particle. The conventional techniques that are typically used for the solar power forecasts are multiple linear regressions, stochastic time series, general exponential smoothing, state space, Kalman filter, as well as the artificial neural network techniques [44].

Many short-term forecasting models for solar power were proposed in the literature. Most of the accomplished works in the short-term forecasting models for PV systems were presented for solar radiation forecasting [43],[45], while few works were designated for models were oriented directly to solar power predictions in PV systems [46],[47]. A Support vector machines (SVM) has been proposed in [47] to predict the hourly PV power generation for a horizon of 24 hrs. Another proposed SVM model in [48] has shown that SVM has better ability in the dealing with the time-varying and nonlinear nature of the solar data over the autoregressive (AR) model and the radial basis function neural network (RBFNN) model. In these work, several forecasted weather variables (such as cloudiness, temperature, etc.), were used as inputs to the model. Genetic programming of fuzzy rules has been described in [49] to forecast the output of a PV plant. The previous proposed models only provide the electric power point forecasts. While a proposed model in ref. [46] provides uncertainty values of the point forecasts. This model allows the evaluation of the risk associated with forecasting errors. Uncertainty values are important in electricity markets because forecasting errors may lead to economic penalties.

A novel hybrid model for PV power forecasting has been proposed in [50]. It combines ARIMA, SVM, artificial neural network (ANN), and adaptive neurofuzzy inference systems (ANFISs) methods with GA algorithm. It showed that the hybrid prediction model provides the most accurate predictions.

2.3.2. Wind Power Modeling

Wind energy is one of the most promising green energy sources. However, wind has complex and stochastic nature, and the generated power from wind turbine is a function of direct wind speed fluctuations. Therefore, accurate wind power forecasts are necessary for the economics of wind energy utilization and power system reliability. Wind power forecasts may be performed at various time scales, depending on the application. The prediction horizon may range from few minutes up to a few days or even few months. It can be divided into two parts: short-term or long-term forecasting. Short-term forecasting is used to predicting wind speeds or wind power few minutes, hours or days. Long-term forecasting includes predictions for several days, weeks or months [51]. Wind power forecasting improvements may be achieved by using more data and providing uncertainty estimates alongside the predicted values [52].

Current approaches of wind speed forecasting generally fall into two main categories. One is the physical model approach and the other is the time series model approach. The first approach, not only considers historical data but also the meteorological conditions and wind turbines information (power curve, hub height, etc.). Physical models are usually better for long-term forecasting (6 hours ahead or more) and it does not fit short-term prediction because of the difficulty of data acquisition and the complexity in computation [53]. Physical modeling requires wide and deep knowledge about atmospherics and is difficult to set up and maintain [54].

On the other hand, the time series model approach only uses historical data to establish the prediction. This approach fits only short-term forecasting (<2 hours ahead) because of the existence of a correlation between consecutive wind speeds where studies of wind speed behavior confirmed this phenomenon [61]. Modeling of the historical wind speed data is done based on statistical theories. The future value is predicted by using the existing time series model and the recent past values. The simplest method of this kind in which the predicted wind speed in the next time slot is the last measured one. More advanced techniques are the ARMA models, Kalman Filters, ANN, Fuzzy Logic and a hybrid prediction based on wavelet transformation and ARMA [53].

A proposed model in [55] is based on a discrete time Markov chain models of order one and two. It allows to directly estimating the wind power distributions on a very short-term horizon. The models are compared to those Models of ability to evaluate the prediction errors associated with the predicted values.

The previous two approaches have limitations. Therefore, some researchers have combined physical and statistical models which results in a hybrid models, as in refs [56],[57], by using Numerical Weather Prediction (NWP) data as inputs to a statistical model. i.e. ref. [54] investigated a combination of numeric and probabilistic models in one-day-ahead wind power forecasts by the Gaussian Processes (GPs) applied to the outputs of a NWP model.

Wind power generation modeling methods are divided into two approaches: the wind speed approach [51], [57] and the wind power approach [54]-[56], [58]. Both of them basically depend on wind speed measurements. But the wind power generation falls between the lower and upper limits of WT power curve and does not follow a standard probability distribution. This increases the difficulty to apply standard statistical models in the wind power approach. On the other hand, a small error in the wind speed modeling in the wind speed approach leads to a large error in the predicted wind power. This is due to the cubic relation between the generated wind power and the wind speed [58].

2.3.3. Energy Storage Application

Global warming is one of the biggest problems in the world, should be taken into account. In trying to mitigate these fears, it is known that using of renewable energy sources has potentially become very important in reducing the emissions of harmful gases ($CO2$, NOx, SOx). But the electricity generation from the most renewable energy resources (RER) is always fluctuated due to their intermittent nature that depends on the environmental status. The variability of renewable energy and its impact on the power system reliability are major challenges stand in its increased penetration. On the other hand, controlling production and controlling demand options could be applied as solutions for the aforementioned problems and ensuring balance between production and demand. However, with existence of fluctuating energy sources, flexible demand has shown little ability [4].

The remaining option in which these fluctuations can be suppressed in the most effective manner is by utilizing an energy storage system [5]-[7]. Energy storage will play a key role in decarbonizing the electricity systems worldwide [8]. And recent developments in energy storage and power electronics technologies will increase the application of energy storage technologies and make it a potentially suitable solution for modern power systems to be operated in a more flexible, controllable manner. Using of energy storage technologies eases the scheduling of renewable energy generation that plays a main role in increasing the penetration of renewable energy globally. Add to this, existence of energy storage in a supply system enables the decoupling of electricity generation from load. In other words, the electricity that can be generated from intermittent RER or at times of low-demand is shifted in time to be released at times of high-demand or when there is a lack in the generated electricity. Therefore, energy storage has strong ability in reducing the imbalance in power and mitigating voltage rise problems due to the stochastic intermittence in the renewable power. In this way, energy storage facilitates the integration of renewables, enhances the efficiency of transmission and distribution networks (reduce grid congestion, frequency and voltage fluctuations), increases the level of de-carbonization of the electricity grid [9].

Energy storage systems for a long time have been utilized in many forms and applications. Nowadays, energy storage technologies are used to achieve electric power systems of higher reliability with enabling a broader use of renewable energy [59]. using of energy storage introduces many benefits including time shifting, peak demand shaving, generation efficiency improvement, and transmission capacity utilization improvement, etc. There are many power system applications where storage is important, with different requirements such as response time, energy and power capacities; i.e., the time scales may range from microseconds (power quality, frequency response) to months (seasonal storage). Thus, no single energy storage technology will be the best for all power applications [60].

Energy storage technologies can be mainly categorized into three groups: mechanical, electromagnetic and electrochemical storage [59]. The first group combines compressed air energy storage, pumped hydro storage and flywheels. Electromagnetic storage includes superconducting magnetic storage and super-capacitors. Electrochemical storage includes hydrogen energy storage and all batteries types. The storage technologies are also grouped with respect to the storage capacity. Because storage capacity can be used to exclude those sizes not suitable to the renewable energy systems [61], [62]. As well as different energy storage technologies have a wide range of discharge rates that ranges from few seconds to hours and even days [62].

Regarding to their capacity, energy storages can be divided into short-term and long-term energy storages [59]. In the short term, the storage is used between the ramping down time of wind and solar plants and the ramping up time of these plants as well as it is used to stabilize the frequency and voltage of the grid [8]. Short-term storage systems include the supercapacitor energy storage, flywheel energy storage and superconducting magnetic energy storage. The long-term storage systems are used in the energy management and energy compensation. It includes pumped hydro energy storage, compressed air energy storage, battery energy storage, and hydrogen energy storage [59].

Energy storage can be integrated at different levels: [8]

1. Generation level: balancing and reserve power, etc.
2. Transmission level: frequency control.
3. Distribution level: voltage control, capacity support, etc.
4. Customer level: peak shaving, time shifting, etc.

Each location will contribute to the reliability and availability of the power and increase the share of renewable energy in electricity system.

Several ES models have been proposed to decrease the impact of RER such as Wind and sun. i.e., in [41], the reliability evaluation of the small stand-alone RE systems has been proposed. It has proposed approach to enhance WP system reliability in distribution network by incorporating ESS. It has explained procedure to determine the ES capacity and charging/discharging power ratings for different operating strategies. And ref. [63] proposed a stochastic framework to determine the optimal sizing of ES. The study used SMCS alongside with search-based optimization technique to minimize the system cost and satisfy reliability requirements.

Many papers researched the community ES (CES) which is located near the customer side. It is considered the best ES to mitigate the impacts of RES at the grid edge [64]. Several works considered the CES, i.e. in [65], proposed an energy management system (EMS) that facilitates the CES in distribution system with high RE penetration and electrical vehicles (EV). The proposed EMS was developed to determine the optimal dispatch level for CES to reduce the demand during peak hours. Refs. [66]-[68] show that using CES in distribution systems help generate electricity without emission and may reduce its production cost. Ref. [68] argues that single phase ES near to customer side in form CES is more efficient in reducing the production cost of electricity than the three phase storage at the substation or street. In [69], a proposed method that shows CES can solve the voltage violation in distribution network with PV integration. However, ref. [67] argues that CES cost a large amount of money which should be taken into account.

The main gap, that this thesis discusses and fills, is using the smart restoration and energy storage to improve the reliability of MG under the case of stand-alone and full penetration of renewable energy.

Chapter 3

MODELING AND PROBLEM FORMULATION

3.1. Introduction

In this thesis, the solar energy and wind energy are considered as the main sources in the microgrid that are used to power the microgrid's load. These two sources can be connected directly to the load point or connected to a feeder to serve several load points. In this thesis, the two connections have been examined.

The autoregressive moving average (ARMA) model is used in this thesis to model the short-term forecasting of wind speed. It uses a historical wind speed data for a wind site in Ottawa, Canada [70]. The output wind power is then computed by using the power-wind speed curve. Solar power is modeled by using the triple exponential smoothing method. This method is very useful when the most recent values contain the most information are needed for short-term predictions. The system load are represented by hourly load curve for one year. The energy storage system is modeled as a dispatchable source model.

3.2. Solar Power Modeling

In the short-term forecasting of the solar power, the most recent values contain the most information needed for predicting the solar power in the near future. Therefore, exponential smoothing methods can be used. Since solar power data contains trend and seasonal features, triple exponential smoothing model is used.

3.2.1. Triple Exponential Smoothing Model

Solar power data involves trend and seasonal features, which establishes the application of triple exponential smoothing method to model the data. In this method, a third smoothing parameter is added to take care of the seasonality. The formula of the triple exponential smoothing model is expressed in the following equations [43]:

$$F_{t+1} = \alpha(D_t - S_t) + (1 - \alpha)(F_t + T_t) \tag{3.5}$$

$$T_{t+1} = \beta(F_{t+1} - F_t) + (1 - \beta)T_t \tag{3.6}$$

$$S_{t+1} = \gamma(D_t - F_{t+1}) + (1 - \gamma)S_t \tag{3.7}$$

Where S_{t+1} is the seasonal value of the next period. S_t is the seasonal value of the present period. γ is the smoothing constant of the seasonality. Equation (3.5) takes care of the estimated value. Equation (3.6) provides smoothing for the trend and (3.7) takes care of the seasonality.

Then the forecast is obtained by adding the outputs of the previous equations as in (3.8):

$$SAF_{t+1} = F_{t+1} + T_{t+1} + S_{t+1} \tag{3.8}$$

Incorporating uncertainties in the reliability study introduces the worst scenario that could happen, which allows the system operator to prepare and account for. Several models have been proposed to incorporate the uncertainty in the power source [71]. In this thesis, the uncertainty in the power source has been incorporated by using the mean absolute percentage error (MAPE). This index indicates the uncertainty percentage in the power source. It is computed by finding the cumulative absolute difference between the actual values and forecasted values divided by the total sum of the actual values. As the uncertainty increases, the MAPE increases. For example, if the MAPE has been found 0.1095 in the solar power and 0.2224 in the wind speed for a prediction horizon of 1 hour, this means that the actual PV or wind speed outputs would swing up or down by 0.1095 or 0.2224 at most of the predicted outputs, respectively.

If the forecasted PV output is $\breve{p}$ and MAPE is e, then

$$p_{pv}^{max} = \breve{p}(1 + e) \tag{3.9}$$

$$p_{pv}^{min} = \breve{p}(1 - e) \tag{3.10}$$

Where $p_{pv}^{max}, p_{pv}^{min}$ are the maximum and minimum limits of the expected PV output, respectively.

Then, the new expected PV output is given by (3.11)

$$p_{pv} = p_{pv}^{min} + rand * (p_{pv}^{max} - p_{pv}^{min}) \tag{3.11}$$

Where $rand$ is a uniformly distributed random number in the interval [0,1]. p_{pv} is the expected PV output.

3.3. Reliability Analysis of Solar Power System

In reliability analysis, RAMS is an abbreviation for Reliability, Availability, Maintainability and Safety and aims to suggest an integrated and methodological approach to deal with system dependability. The fundamental objective of the RAMS analysis is to pinpoint the system failure causes and its components [72].

Many functions are used in the RAMS analysis such as the failure density function, reliability function and failure cumulative distribution function, etc. The components in power system are typically assumed to have constant failure rate during their life cycle as the past of the power systems certifies this fact. Therefore, the failure density function should be exponentially distributed. The reliability function is then expressed with respect to the random variable ***T*** as follow:

$$R(t) = P(T \geq t, succeeds) = \int_t^{\infty} \lambda e^{-\lambda\tau}\, d\tau = e^{-\lambda t} \tag{3.12}$$

This function represents the probability of a component or system to survive greater than or equal to time t. While the failure distribution function is the probability of a component or system to fail during certain period of time or less than or equal to time t.

$$F(t) = P(T \leq t, fails) = \int_0^{t} \lambda e^{-\lambda\tau}\, d\tau = 1 - e^{-\lambda t} \tag{3.13}$$

The instantaneous failure rate (Hazard rate) is the probability of a system or component to fail between time *t* and *t + dt*, given it is operating at time t. It is computed by inversely deriving *R(t)* with respect to the time divided by *R(t)* as,

$$\lambda(t) = -\frac{1}{R(t)} . \frac{dR(t)}{dt} = -\frac{\dot{R}(t)}{R(t)} \tag{3.14}$$

Since the failure rate of the power system components is constant, therefore

$$\lambda(t) = \lambda$$

There are several techniques are used to perform the reliability analysis. Among these techniques, the quantitative analysis techniques which are based on the modeling of the physical and logical connections between system components and doing the reliability analysis using statistical methods. Series/parallel system reliability analysis is one of these techniques that is widely used. According to this technique, the series system has a normal state at time t, if and only if all its components are found in upstate at time t. While in the parallel model, the system is considered in normal state at time t, if and only if one or more of its components are found in upstate at time t. In power system, the failure of the component is independent from the others. Therefore, the reliability of a series system of n components can be evaluated as,

$$R_s(t) = \prod_{i=1}^{n} R_i(t) = \prod_{i=1}^{n} e^{-\lambda_i t} = e^{-\sum_{i=1}^{n} \lambda_i t} \tag{3.15}$$

Whereas the reliability of a parallel system can be evaluated by (3.16),

$$R_p(t) = 1 - F_p(t) = 1 - \prod_{i=1}^{n} (1 - e^{-\lambda_i t}) \tag{3.16}$$

Typically, the photovoltaic (PV) system consists of four main components [72] as shown in Fig. 3.1.

1) PV generator: it consists of a group of solar panels (SP), each panel combines a set of interconnected solar cells. Each cell converts the sunlight into DC current at certain

voltage. The panels are connected to form array to provide the desired voltage and current.

2) Inverter: it converts the DC voltage into a desired AC voltage.

3) Energy meter: it is a measurement device that measures the produced electrical energy from PV generator. It also can be used to identify the PV system performance.

4) Electrical boxes: these boxes are used to connect the system components and provide the required protection against the short circuits and peaks voltage.

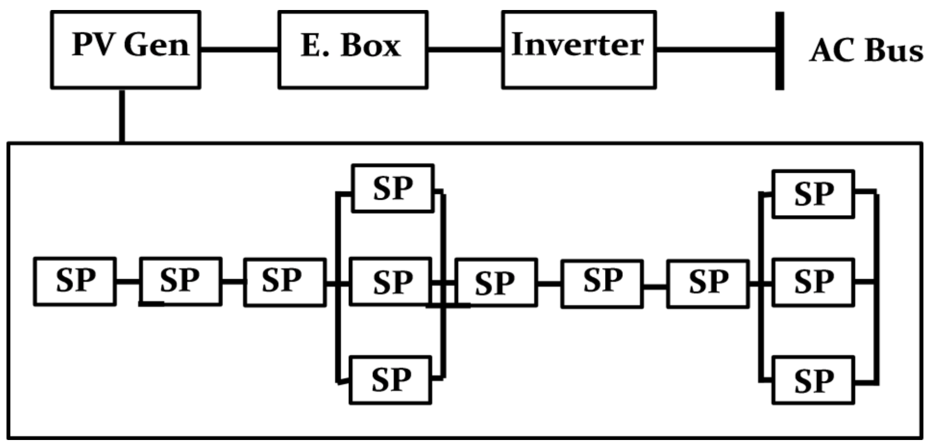

Fig.3.1 Reliability block diagram of the PV power plant

The above components are always connected in series configuration as in Fig. 3.1. This results in a series system whose reliability model can be evaluated as,

$$R_{PV}(t) = R_G * R_{box} * R_{Inv} \tag{3.17}$$

Where R_G is the reliability of the PV generator. $R_{box}$is the reliability of the electrical boxes. R_{Inv} is the reliability of the inverter. The reliability of each part can be expressed by using equation (3.15) or (3.16) or both as,

$$R_G = e^{-\sum_{i=1}^{SP_{series}} \lambda_{SP_i} t} * \left(1 - \prod_{j=1}^{SP_{parallel}} \left(1 - e^{-\lambda_{SP_j} t}\right)\right) * \left(1 - \prod_{j=1}^{SP_{parallel}} \left(1 - e^{-\lambda_{SP_j} t}\right)\right) \quad (3.18)$$

$$R_{box} = e^{-\lambda_{box} t} \quad (3.20)$$

$$R_{Inv} = e^{-\lambda_{Inv} t} \quad (3.21)$$

If all the panels have the same λ_{SP} and each parallel part has the same number of SPs, (3.18) becomes,

$$R_G = e^{-SP_{series} \lambda_{SP} t} * \left[1 - \left(1 - e^{-\lambda_{SP} t}\right)^{SP_{parallel}}\right]^2 \quad (3.19)$$

Where SP_{series} is the number of SPs that are connected in series. $SP_{parallel}$ is the number of the parallel SPs in each part. λ_{SP} is the failure rate of the SP. λ_{box} is the failure rate of the electrical box. λ_{Inv} is the failure rate of the inverter.

3.4. Wind Speed Modeling

The existing wind power generation modeling methods are divided into two approaches: the wind speed approach [51],[57] and the wind power approach [54]-[56],[58]. Both of them basically depend on wind speed measurements. The wind speed approach has been used in this thesis for modeling and forecasting the short-term forecasting of the wind speed by using the autoregressive moving average (ARMA) model.

The model is usually called the ARMA (p,q) model where p and q are the orders of the autoregressive part and the moving average part, respectively. The autoregressive integrated moving average (ARIMA) is similar to ARMA but it uses a third parameter that defines the order of the integration when the time series follows a non-stationary stochastic process. This model is usually written as ARIMA (p,d,q) and d is the order of the integration.

The autoregressive model of order p for a certain time series X(t) can be expressed as,

$$X(t) = \sum_{i=1}^{p} \alpha_i X(t-i) + e(t) + c \tag{3.22}$$

and the moving average model of order q can be written as,

$$X(t) = \sum_{i=1}^{q} \beta_i e(t-i) + e(t) \tag{3.23}$$

Thus, ARMA(p, q) consists of the two models, AR(p) and MA(q) as,

$$X(t) = \sum_{i=1}^{p} \alpha_i X(t-i) + \sum_{i=1}^{q} \beta_i e(t-i) + e(t) + c \tag{3.24}$$

Where $\alpha_1, \dots, \alpha_p$ and $\beta_1, \dots, \beta_q$ are the coefficints of the AR(p) and MA (q) respectively. c is the constant term. $e(t)$ is the error term that is assumed independent identically distributed random variables (i.i.d.) sampled from the normal distribution with zero mean: $e(t) \sim N(0, \sigma^2)$. Where σ^2 is the variance.

In this research, the following four coefficients have been used to validate the model. The Pearson correlation coefficient [73], the mean absolute error (MAE), the root mean square error (RMSE) and the mean absolute percentage error (MAPE) that associated with the original time-series (x) and the forecasted time-series ($\hat{x}$):

$$r_{x,\hat{x}} = \frac{\sigma_{x,\hat{x}}}{\sigma_x \sigma_{\hat{x}}} \tag{3.25}$$

$$RMSE = \sqrt{\frac{1}{N}\sum_{i=1}^{N}(x_i - \hat{x}_i)^2} \tag{3.26}$$

$$MAE = \frac{1}{N}\sum_{i=1}^{N}|x_i - \hat{x}_i| \tag{3.27}$$

$$MAPE = \frac{\sum_{i=1}^{N}|x_i - \hat{x}_i|}{\sum_{i=1}^{N} x_i} \tag{3.28}$$

Where $r_{x,\hat{x}}$ is the Pearson correlation coefficient. N is the number of data points in the original time series, σ_x and $\sigma_{\hat{x}}$ are the standard deviations of x and $\hat{x}$, respectively. $\sigma_{x,\hat{x}}$ is the covariance of the x and $\hat{x}$:

$$\sigma_{x,\hat{x}} = \frac{\sum_{i=1}^{N}(x - \mu_x)(\hat{x} - \mu_{\hat{x}})}{N} \tag{3.29}$$

μ_x and $\mu_{\hat{x}}$ are the mean values of x and $\hat{x}$, respectively.

The uncertainties in the wind speed can be included using the same procedure that has been explained in the solar power modeling. Then, the wind power output is given by the power curve, it is expressed as [74],

$$P(v) = \begin{cases} (A + B * v + C * v^2)P_r & v_{ci} \le v \le v_r \\ P_r & v_r \le v \le v_{co} \\ 0 & otherwise \end{cases} \tag{3.30}$$

The V_{ci}, V_r and V_{co} are the cut-in, rated and cutout wind speeds in (m/s), respectively. P_r is the rated power of the WTG in MW. v is the wind speed. A, B and C are constants and can be calculated using the following equations [74],

$$A = \frac{1}{(v_{ci} - v_r)^2}\left[v_{ci}(v_{ci} + v_r) - 4(v_{ci}v_r)\left[\frac{v_{ci} + v_r}{2v_r}\right]^3\right] \tag{3.31}$$

$$B = \frac{1}{(v_{ci} - v_r)^2}\left[4(v_{ci} + v_r)\left[\frac{v_{ci} + v_r}{2v_r}\right]^3 - (3v_{ci} + v_r)\right] \tag{3.32}$$

$$C = \frac{1}{(v_{ci}-v_r)^2}\left[2 - 4\left[\frac{v_{ci}+v_r}{2v_r}\right]^3\right] \quad (3.33)$$

3.5. Reliability Analysis of the Wind Turbine Generator

The wind farm operates in a modular approach where each turbine operates independently from the other. Each turbine consists of many components that work in series as shown in Fig. 3.2. So for the turbine to work, all components must be working properly.

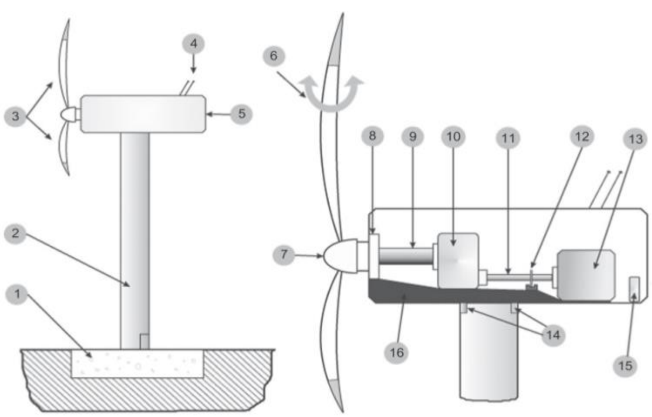

Number	Name	Number	Name
1	Base/ foundations	9	Low speed (main) shaft
2	Tower	10	Gearbox
3	blades	11	High speed shaft
		9+11	Drive train
4	Meteorological unit	12	Brake system
5	Nacelle	13	Generator
6	Pitch system	14	Yaw system
7	Hub	15	Converter
8	Main bearing	16	Bedplate.

Fig.3.2 Components of the WTG: [75]

The reliability block diagram of the complete structure of the WTG is complex. Therefore, a simplified reliability block diagram for the WTG can be represented by the four primary sub-systems in series [76]. They are the blades, gearbox, generator and controls equipment as shown in Fig. 3.3.

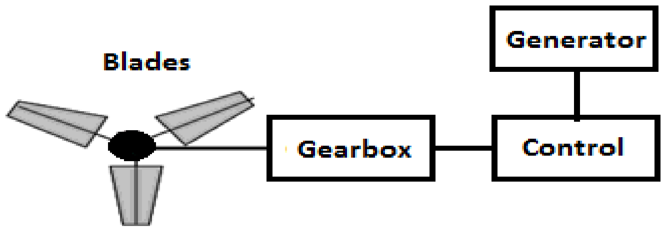

Fig.3.3 Simplified reliability block diagram for the WTG.

The failure rate of any mechanical part, such as the WTG, can be represented as [77],

$$\lambda(t) = \frac{\beta}{\theta}\left(\frac{t}{\theta}\right)^{\beta-1} \tag{3.34}$$

Where β is the shape parameter of the failure function; θ is the scale parameter that represents the time between failures and is greater than 0 for $t \geq 0$.

Fig. 3.4 shows a complete failure curve, the bathtub curve. The three regions can be described by equation (3.34) by using different values for the shape parameter β as follow:

- $\beta < 1$, infant mortality
- $\beta = 1$, normal life
- $\beta > 1$, deterioration or wear out

When $\beta = 1$, the failure rate $\lambda(t)$ becomes constant. Therefore, equation (3.34) can be reduced to

$$\lambda = \frac{1}{\theta} \tag{3.35}$$

Exponential distribution can be used to describe the reliability of wind turbine and its failure probability when the failure rate lies on the normal life region.

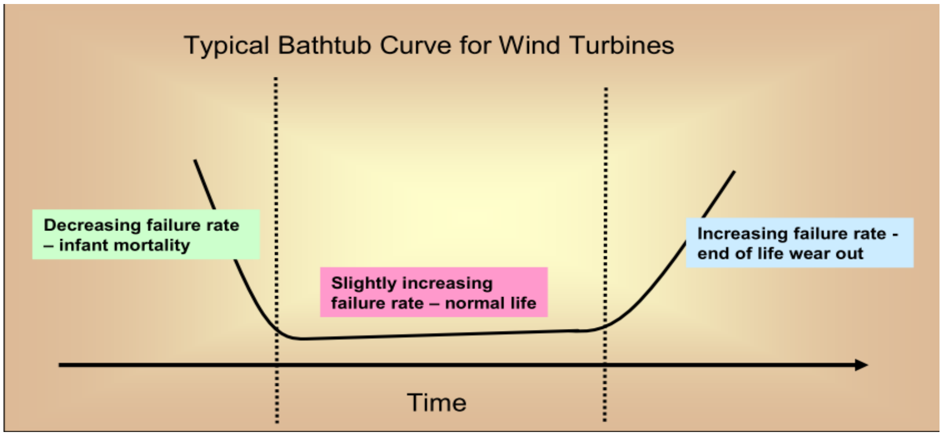

Fig.3.4 Bathtub curve for WTs. [78]

All subsystems of the wind turbine are connected in series as shown in Fig. 3.3. Since the failures of the subsystems of the WTG occur independently from each other; equation (3.15) can be written as,

$$R_s(t) = \prod_{i=1}^{n} R_i(t) = \prod_{i=1}^{n} e^{-\lambda_i t} = e^{-\sum_{i=1}^{n} \lambda_i t} \tag{3.36}$$

$R_s(t)$ is the reliability of the WTG. n is the number of the components or the subsystems of the WTG. λ_i is the failure rate in failure/year per the ith subsystem in the WTG. The failure rate of the WTG can now take the form,

$$\lambda_{WT} = \sum_{i=1}^{n} \lambda_i \tag{3.37}$$

The WTG has two states, operating and failure states. The output power is $P(v)$ when the WTG is in operating state and zero when the WTG is in failure state. Therefore, the reliability model of WTG power output with forced outage rate (FOR) U is summarized in table 3.1:

Table 3.1 Reliability Model of WTG Power Output

State	Capacity (MW)	Probability
1	0	U
2	$P(v)$	$1-U$

Multiple WTGs provide large amount of power and introduce redundancy that increases the availability of the power. The WTGs in wind farm are independent from each other which makes their failures are also independent.

Consider a wind farm of n identical WTGs with rated power P_r MW. Assume that the forced outages of WTGs are neglected, the output power of the wind farm is then $n * P(v)$ MW. If the FOR of each WTG is p, the probability of k WTGs or less to be on forced outage and the probability of m units to be on maintenance are given as [79],

$$P_k = \sum_{i=1}^{k} \binom{n}{i} p^i (1-p)^{n-i} \tag{3.38}$$

$$p_m = \binom{n}{m} p^m (1-p)^{n-m} \tag{3.39}$$

Where $0 \le k \le n$

3.6. Load Modeling

In reliability analysis of power system, accurate load modeling is very important. However, load modeling is not an easy task and time consuming because of many factors such as weather forecast errors, customer behaviors, etc. Therefore, many different load models have been used in reliability evaluation [80]-[82]. The time varying load models of the hourly load variation curve of the RBTS [83] shown in Fig. 3.5 is used in this study. The peak load is 20 MW and average load is 12.3 MW.

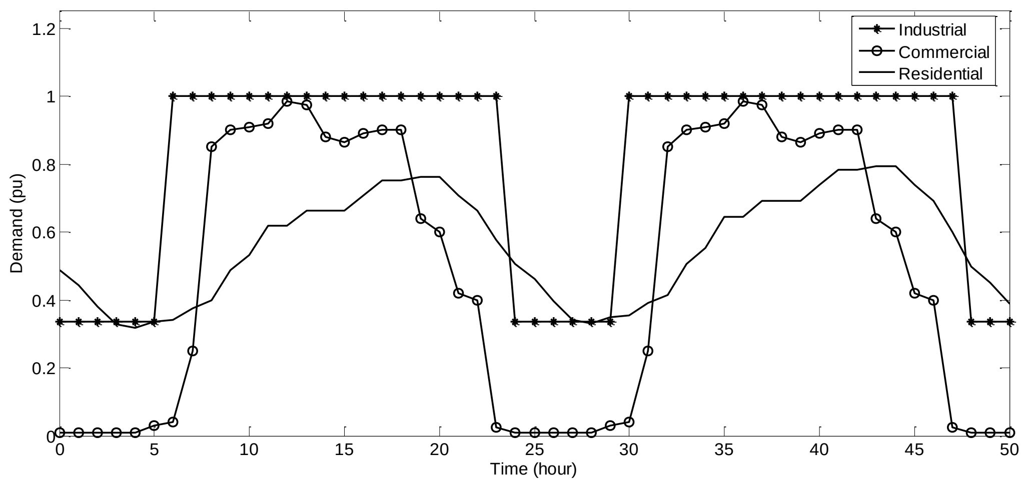

Fig.3.5 The hourly load variation curve of the RBTS system

3.7. Energy Storage Modeling

Energy storage has been used in many power system applications such as peak shaving, time-shifting applications, improving power quality and power system reliability, etc. Hence, many models of energy storage have been presented in literature [84], [85], where it is always modeled as a dispatchable source [86].

Energy storage is a popular option that is used to smooth the output power variations from the intermittent power source, such as wind turbine and PV panels, and provide a stable power output to the grid P_g. i.e., if the power output from the renewable power source $P(t)$ is greater than P_g, the excess power $P(t) - P_g$ is used for charging of the energy storage. The stored energy is discharged when the output power $P(t)$ is less than

P_g. Hence, the charging and discharging power can therefore be calculated from the following two equations:

$$P_{ch}(t) = \begin{cases} P(t) - P_g & P(t) > P_g \\ 0 & P(t) \le P_g \end{cases} \tag{3.40}$$

$$P_{disch}(t) = \begin{cases} P_g - P(t) & P_g \ge P(t) \\ 0 & P_g < P(t) \end{cases} \tag{3.41}$$

In addition, the probability of discharging and charging can be estimated from eqs. (3.42) and (3.43), respectively.

$$\Pr\left(P(t) \le P_g\right) = F_p\left(P_g\right) \tag{3.42}$$

$$\Pr\left(P(t) > P_g\right) = 1 - F_p\left(P_g\right) \tag{3.43}$$

Where the F_p is the power cumulative distribution function of the intermittent renewable source.

The round-trip efficiency of the energy storage indicates to the amount of the energy loss that takes place in one charging-discharging cycle and it is defined as [87],

$$\eta_T = \eta_{ch} . \eta_{disch} \tag{3.44}$$

Where η_{ch} is the charging efficiency. It is defined as the ratio of the charged power to the input power. η_{disch} is the discharging efficiency that provides the ratio of the output power to the discharged power.

The storage device ratings are the main factors that affect the charging and discharging processes. The limited power ratings of the storage device are usually modeled by bounding the charging and discharging equations. With limited power ratings, the charging and discharging expressions should then be modified to, [87]

$$P_{ch}(v) = \begin{cases} \min\left[P(t) - P_g, P_{ch}^{max}\right] & P(t) > P_g \\ 0 & P(t) \leq P_g \end{cases} \qquad (3.45)$$

$$P_{disch}(v) = \begin{cases} \min\left[P_g - P(t), P_{disch}^{max}\right] & P_g \geq P(t) \\ 0 & P_g < P(t) \end{cases} \qquad (3.46)$$

If there is no capacity limit are on charging power, all excess power can be used for charging the storage.

The energy storage is mainly evaluated by four parameters: charging and discharging efficiencies, power and energy capacities. The relationship between the storage state of charge (SOC) and the charging and discharging power P_{ch}/P_{disch} is basically expressed by the following equations: [88]

$$SOC(t+1) = \begin{cases} SOC(t) - \frac{1}{\eta_{disch}} P_{disch}.\Delta t & , \quad Discharging \\ SOC(t) + \eta_{ch} P_{ch}.\Delta t & , \quad Charging \end{cases} \qquad (3.47)$$

$$P_{disch}^{min} \leq P_{disch} \leq P_{disch}^{max} \qquad (3.48)$$

$$P_{ch}^{min} \leq P_{ch} \leq P_{ch}^{max} \qquad (3.49)$$

$$SOC^{min} \leq SOC(t) \leq SOC^{max} \qquad (3.50)$$

In addition, the strategy of operating energy storage also affects the energy storage such as peak load shaving [89], smoothing power output from the WTG or PV panels and priority of the supply source. In this thesis, the energy storage is used to decrease the shortage in the generated power from the WTGs and PV that have priority to supply load. The proposed operating strategy is as follows:

1) If the available wind power or solar power at the current time unit is greater than system load, energy storage will store the excess energy as long as the energy storage limits are not violated. Energy storage cannot always store the available excess energy because of the charging rate limits and the current SOC of the storage.

2) If the available wind power or solar power at the current time unit meets system load exactly, energy storage will not be used.

3) If the available wind power or solar power at the current time unit is less than system load, energy storage will be used to power system load alongside the produced renewable power as long as the energy storage limits are not violated. Energy storage cannot always discharge its stored energy due to the limits of discharging rate of the energy storage and the current SOC in the energy storage.

4) If the available wind power or solar power in the current time slot is less than system load and energy storage cannot compensate the shortage in supply, at this moment the load curtailment will be used to balance supply and load.

5) If the available wind power or solar power at the current time unit cannot be used to power the system load or part of it due to interruptions, the excess energy is stored in the energy storage as long as the energy storage limits are not violated.

In this research, the lower and upper bounds on the $SOC(t)$ are assumed to be 50% and 100% of capacity of the energy storage unit, respectively [86]. Fig. 3.6 shows a model of a grid-connected PV, WTG and energy storage system [85].

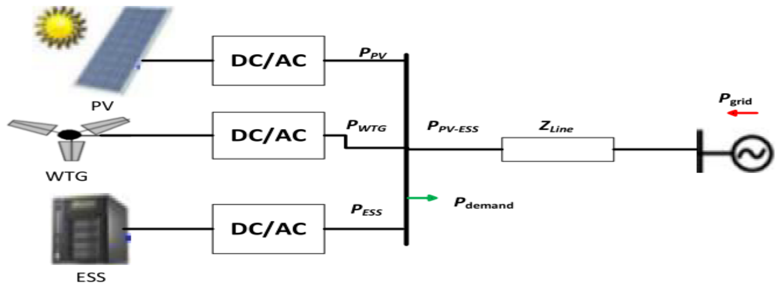

Fig.3.6 Model of a grid-connected PV, WTG and energy storage system.

The reliability model of ESS [72] is shown in Fig. 3.7. It has four states, charge, discharge, standby and down state. Battery will be in discharge state, when demand is larger than production. On the other hand, it is in charge state, when demand is less than supply. EES is in standby state when it is fully charged or discharged. It will be in down state when it is in failure state.

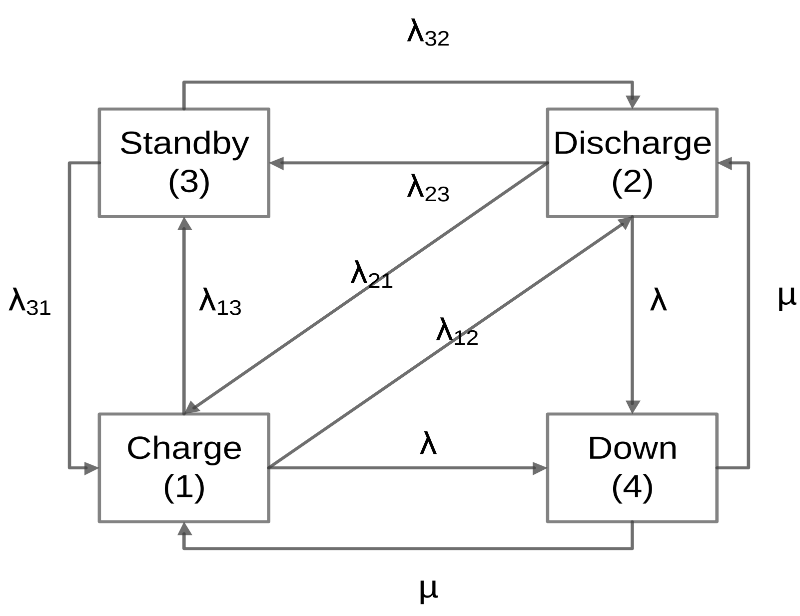

Fig.3.7 State model of energy storage unit

where λ_{xx} is the transition rate between states. λ represents the failure rate. μ is the repair rate.

3.8. Reliability Indices

There are many reliability indices that were proposed in the literature and used in the reliability studies. Expected Energy Not Supplied (EENS) index is the most widely used reliability index in reliability analysis. Calculation of load not supplied is required at every time step in order to compute the value of this index as explained by eqs. (3.51) and (3.52).

$$P_{shed,t} = max\left(0, \sum P_{load,t} - \sum P_{gen,t}\right) \tag{3.51}$$

$$EENS = \frac{\left(8760 \sum_{t=1}^{T} P_{shed,t} * \Delta t\right)}{T} \tag{3.52}$$

Expected energy not used (EENU), is another important index that represents the renewable energy produced but not used and depends on the operating strategy of the renewable sources [90]. The EENU for a certain period of time can be computed by using,

$$P_{excess,t} = max\left(0, \sum\left(P_{gent,t}\right) - \sum\left(P_{load,t}\right) - C + SOC(t)\right) \tag{3.53}$$

$$EENU = \frac{\left(8760 \sum_{t=1}^{T} P_{excess,t} * \Delta t\right)}{T} \tag{3.54}$$

where $P_{shed,t}$ is the amount of the load shedding at time step t. $P_{excess,t}$ is the amount of the excess power at time t. T is the entire period of simulation time in hours. Δt is the time unit in hour. C is the capacity of the available energy storage units. $SOC(t)$ is the state of charge in the energy storage at time t.

Availability (A) of the component or the system is defined as the probability of the component or the system to be in the operating state, while the unavailability (U) is the probability of the component or the system to be in the failure state. These indices can be calculated from (3.55) and (3.56),

$$A = \frac{\mu}{\mu+\lambda} = \frac{uptime}{uptime+downtime} \tag{3.55}$$

$$U = \frac{\lambda}{\mu+\lambda} = \frac{downtime}{downtime+uptime} \tag{3.56}$$

System average interruption duration index (SAIDI) provides the expected amount of down time that each customer will experience in average during a certain period of time and can be calculated using (3.57),

$$SAIDI = \frac{Total\ duration\ of\ all\ interruptions}{Total\ number\ of\ customers\ connected} \tag{3.57}$$

System average interruption frequency index (SAIFI) provides the expected number of failures that each customer will experience during a certain period of time and can be calculated using (3.58),

$$SAIFI = \frac{Total\ number\ of\ all\ interruptions}{Total\ number\ of\ customers\ connected} \tag{3.58}$$

The previous indices evaluate the reliability of the system. While the average down time and failure frequency can be used as load indices. Average down time provides the amount of time per failure on average while the failure frequency provides the number of failures that the load point experienced during 1 year. They can be calculated using (3.59) and (3.60),

$$Downtime\ per\ failure = \frac{U_{LP}}{N_{LP}} \tag{3.59}$$

$$Failure\ frequency = \frac{N_{LP}}{n} \tag{3.60}$$

Where U_{LP} is the unavailability of the load point in hours. $N_{LP}$is the total number of failures and n is the number of years.

3.9. Monte Carlo Simulation and Smart Restoration of Electric Microgrid

3.9.1. Monte Carlo Simulation for Smart Restoration

Monte Carlo simulation is a computerized mathematical technique that performs risk and decision making in quantitative analysis. MCS is characterized as a sampling method because the inputs are generated and selected randomly from probability distribution to simulate a sampling process from actual population.

MCS is able to translate the input uncertainties to uncertainties in the system outputs to show the impact of the input uncertainties on the outcomes, as well as it allows us to explore the all possible outcomes by which we can determine the likelihood of each outcome and estimate the probability. MCS procedure can vary from one form to another based on the system under study. However, MCS procedure for any system in general should pass through the five steps listed below,

1) Create a parametric model, $y = f(x_1, x_2, \dots x_q)$
2) Generate a set of random inputs, $x_{j1}, x_{j2}, \dots x_{jq}$
3) Evaluate the model and record the results as y_i
4) Repeat steps 2 and 3 for $i = 1\ to\ n$
5) Analyze the results using histograms, confidence intervals, etc.

MCS is used to evaluate the reliability of power supply and load availability. It helps in estimating the expected energy curtailment and loss of load expectation (LOLE). Also, the frequency and the likelihood can be estimated for each system state over certain period of time.

In this thesis, MCS is used to evaluate and analyze the reliability of MG and the impacts of smart restoration on the reliability. Fig. 3.8 shows a flowchart that explains the process of computing some of reliability indices such as the availability, the duration and number of failures, the down time and the failure frequency of each load point (LP) by MCS. The steps are explained as follows,

Step 1. Collect the mean time to failure (MTTF) and the mean time to repair (MTTR) of each component.

Step 2. Generate two random numbers uniformly distributed (u_1, u_2) for each component.

Step 3. Convert u_1 to time to failure (TTF) and u_2 to time to repair (TTR) by using the inverse transform method:

$$TTF = \frac{1}{MTTF} ln(u_1) \tag{3.61}$$

$$TTR = \frac{1}{MTTR} ln(u_2) \tag{3.62}$$

Step 4. Form an array (D) of size 1 x (TTF+TTR) for each component that consists of ones and zeros.

Step 5. Repeat step 2 to 4 until the size of D equals number of hours in n years.

Step 6. Perform the "And" operation and store the result in array T.

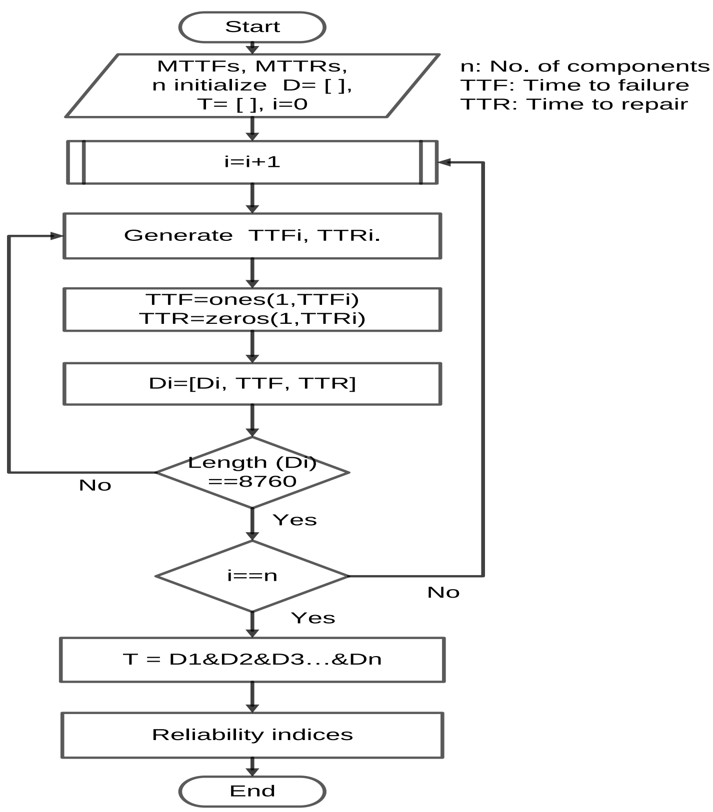

Fig.3.8 Flowchart of evaluating Reliability indices of a LP by MCS

3.9.2. Smart Restoration of Electric Microgrid

The main function of smart restoration is to locate and restore the interrupted loads based on their priorities. It has the capability of optimizing the sequence of switch operations. Implementing smart restoration allows the distributed generation (DG) resources and associated ESS units to be operated efficiently and strategically. Hence, smart restoration is able to improve the reliability and allow a large deployment of the renewable energy sources (RES).

In this thesis, the smart restoration system is implemented such that the stand-alone microgrid system can be in one of three states as shown in Fig. 3.9. The power system will be in the normal state when all equipment works within their limits. It will be in failure state when there is a major outage in generation or customer load. The restorative state takes place when the system restores the isolated area from major failure by using the backup resource, such as ESS. The restorative state has been designed to return the system back to the normal state, but could accidentally take the system again to failure state. The general process of the smart restoration for islanded system is shown in Fig. 3.10.

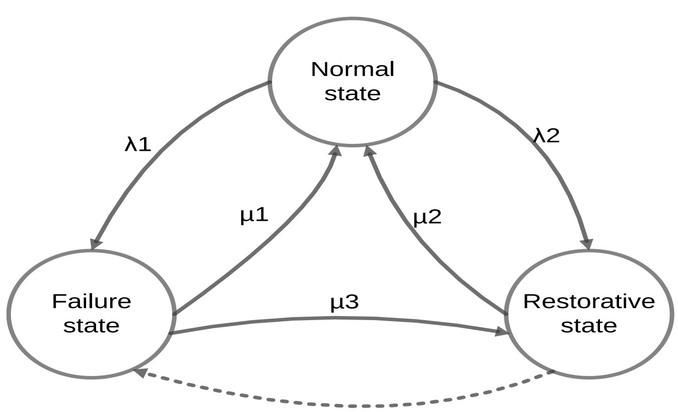

Fig.3.9 States of the MG

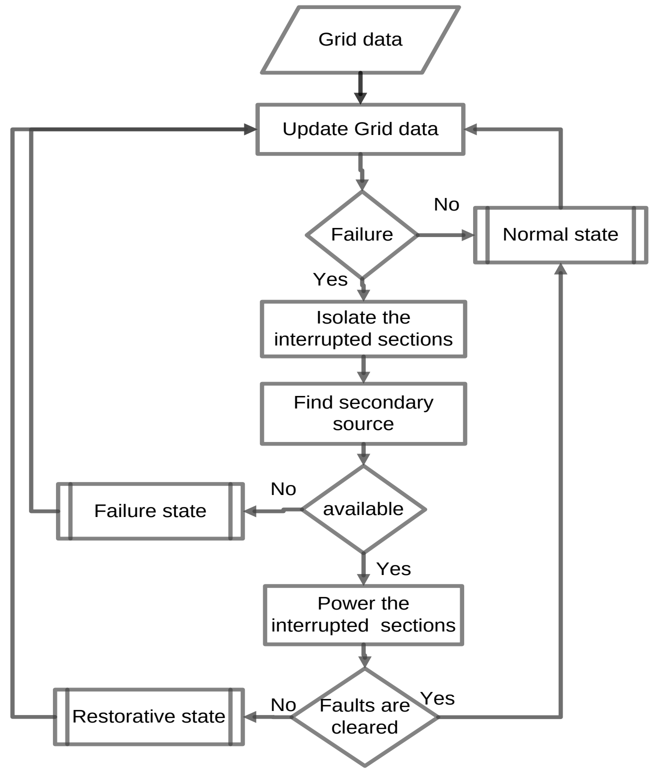

Fig.3.10 General flowchart of smart restoration

The system applies smart restoration to recover the MG from a failure state and uses the stored or the excess energy from the neighbors. Smart restoration assumes load priority separately in each one of the four sections of the MG, with the capability of changing these priorities. These priorities are as follow:

MG1: 1-2-5-4-3-6-7.

MG2: 8-9.

MG3: 12-11-14-10-15-13.

MG4: 16-18-17-20-19-22-21.

If the demand of the microgrid is greater than the supply or if there is a failure, the smart restoration looks for DG to serve the load. Then, if the load is not served, smart restoration looks for DGs or ESS in the other MGs and reconfigures the whole MG to transfer the power to the interrupted load. This process is explained in Fig. 3.11.

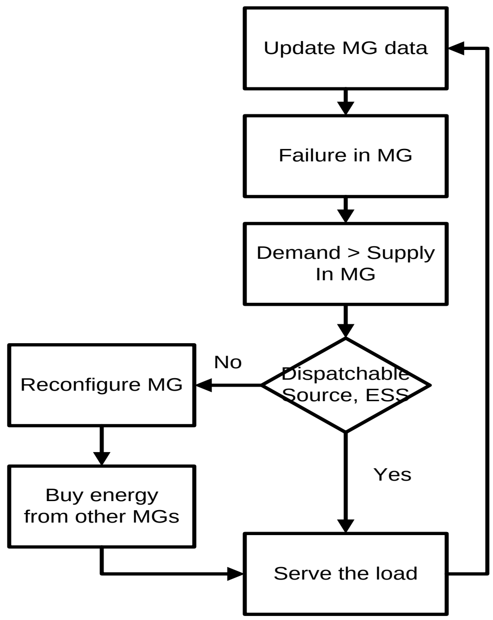

Fig.3.11 Flowchart of smart restoration operation when demand is greater than supply

When the demand in the MG is less than the supply, the ESS will be charged. If it is not possible, smart restoration reconfigures the MG and sells the energy to the other MGs as explained in Fig. 3.12.

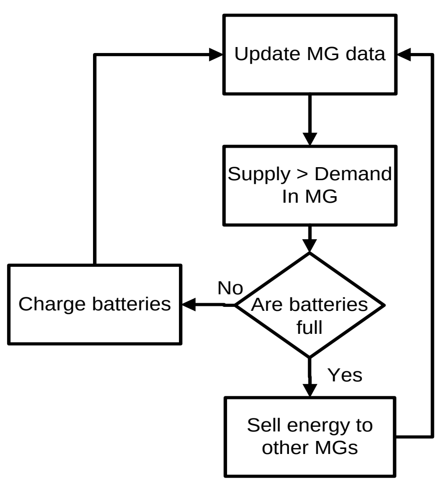

Fig.3.12 Flowchart of smart restoration operation when demand is less than supply

Fig. 3.13 shows hourly load profile of a load point in MG. The top curve in Fig. 3.13 shows that outages occurred due to failures or shortage in power. After using smart restoration, the load is served by using the batteries or transferring the power from other MGs.

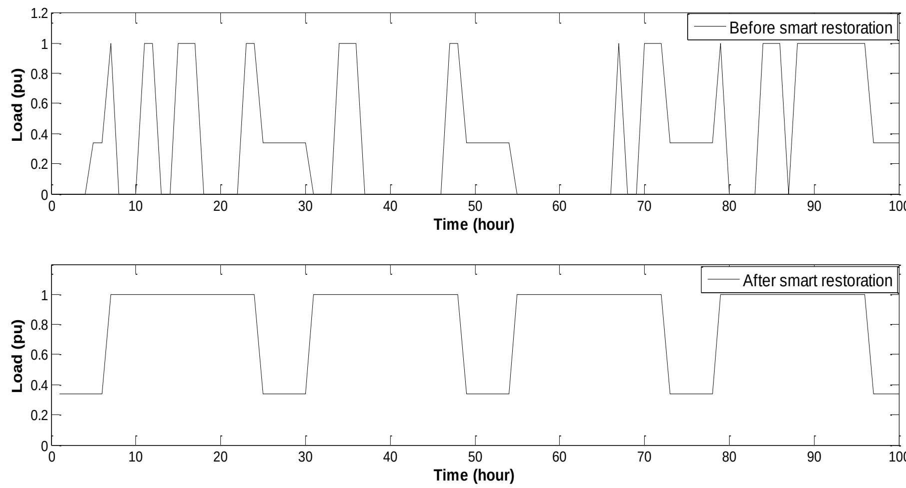

Fig.3.13 hourly load profile of a load point in MG

In this study, the wind and solar power units are installed at the green places in the RBTS system as shown in Fig 3.14. LP and T in the figure mean load point and topology, respectively. The selected places have been chosen based on this reason, the place that is the nearest to the biggest number of customers. For example, the intersection point of transmission line 5 and 6 in MG 1 has been selected as the targeted place for the power source. This point is approximately the most point near to all load points in MG 1. If any other point is selected, it will not be near to all points in MG 1. The simulation considers three cases in each MG. Case 1 uses the wind power only at the specified places. The solar power is used in Case 2. Case 3 uses the wind and solar power at the same time and assumes that their capacities are equal.

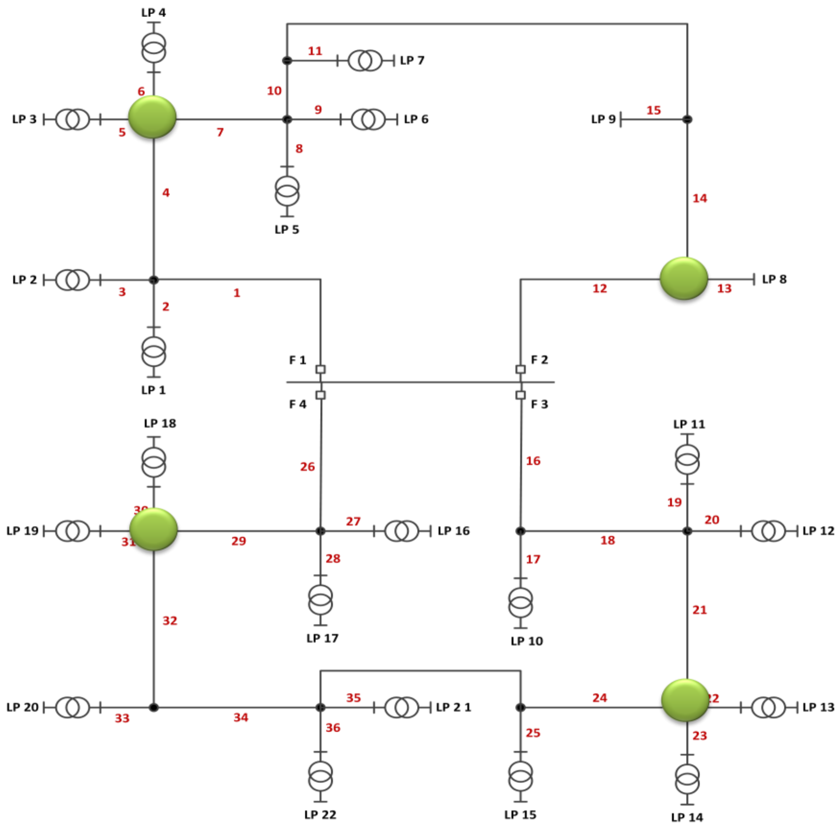

Fig.3.14 Single line diagram of RBTS system

The capacity of the wind power or the solar power in each section ranges from 5-25 MW. Smart restoration is used in the all cases and it works when a failure or power shortage happens. It tries to restore the interrupted load points by looking for another route or transferring the power from the neighboring MGs or using the stored energy. Each case is simulated with and without the smart restoration. Both cases use the energy storage and assume existence of the uncertainty in the renewable power supply. In each case, the system runs the simulation and computes the reliability indices. The RBTS bus 2 is divided into four MGs, each one has its own load priority list as shown in Fig 3.15.

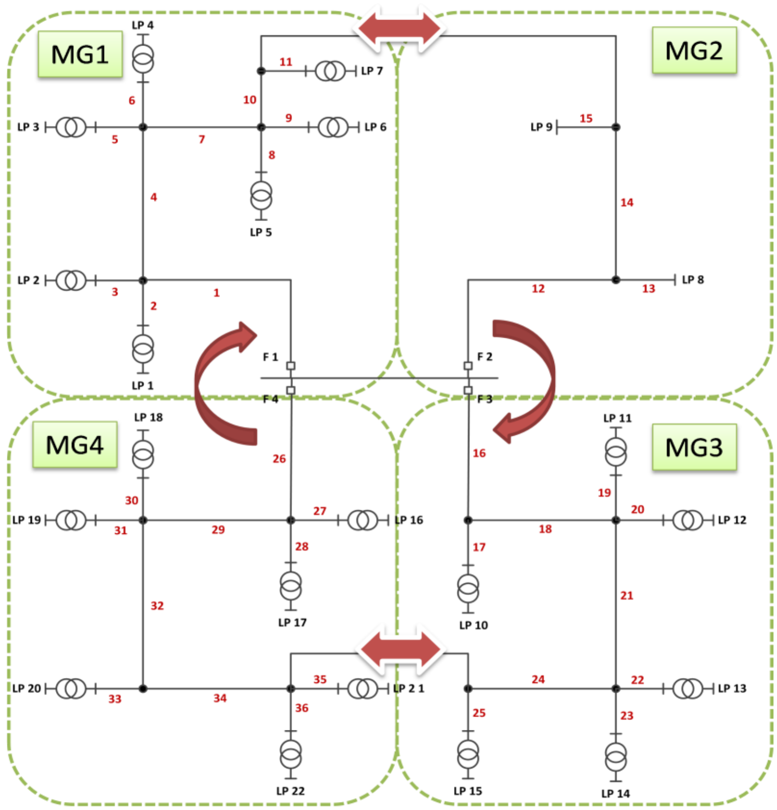

Fig.3.15 Power flow diagram in the RBTS system

After using the smart restoration, the RBTS bus 2 can be viewed as a ring topology with multiple power sources. The MGs are connected to each other through switches. The switch has two states: normal and down states. When the power in the MG is not enough, the smart restoration looks for energy storage or another path to restore the load point by using the excess generated power in the neighbors. If there is a failure that separates the load point from the grid and there is no possible path for the power to pass through, the load point will experience a permanent failure unless there is storage near the load point as illustrated in Fig 3.10. The imported power from the neighbors can pass through the bus 2 or through the switches on the ring path, as shown in Fig. 3.15.

3.9.3. Resources Scheduling in Microgrid

Scheduling of the resources is very important. It optimizes the usage of the resources and makes the MG withstands the interruption in better way. The scheduling is utilized by the smart restoration by considering how much energy will be in the next time unit to optimize the operation of MG. For example, if the generated energy from the wind in the next two hours is expected to be 2 and 0.5 MW in MG 1 and the total load is expected to be 6 and 6.5 MW. If the current SOC in the ESS is 14 MWh and the SOC^{min} is 10 MWh. If there is a dispatchable generator of capacity of 8 MW and ramping rate of 4 MW has not been started yet. Moreover, the supply in the other MGs is expected to be less than the demand in the next two hours. In this scenario, smart restoration has five choices to cover the shortage in the coming two hours. First choice is discharging the ESS at rate 4 MW. It cannot be used because it is unable to cover the shortage in the second hour due ramping rate of the generator. The second one is starting dispatchable generator at rate 4 MW. It is expensive because it operates the generator at 4 MW in the first hour and 2 MW in the second hour and does not use the ESS in the first hour. The third choice is discharging ESS at rate 3 MWh and operating the generator at rate 1 MW. It is also expensive because it operates the generator at 1 MW in the first hour and at 5 MW in the second hour. The fourth choice is discharging ESS at rate 2 MW and operating the generator at 2 MW too. In this choice, the generator operates at 2 MW in the first hour and at 4 MW in the second hour which is expensive too. The last choice is discharging ESS at 1 MW and operating the generator at 3 MW. This choice is the cheapest choice where the generator operates at rate of 3 MW in the two hours and uses all the energy in the ESS that can be drained.

Another example, if the next hour is the hour 201 in the Fig. 3.16 that shows the total demand and supply in each MG in Fig. 3.15. The forecasted demands in MG 1 and MG2 are 5 and 2 MW that exceed the forecasted supply which are 4 and 1.2 MW respectively, while the supply exceeds demand in MG 3 and MG 4. Also the SOC reached the SOC^{min}. In this case, smart restoration reconfigures the whole MG to cover the shortage in MG 1 and MG 2. It will transfer the power from MG 3 and MG 4 through the common bus and cover the shortage in MG 1 and MG 2 if this forecasted action happened.

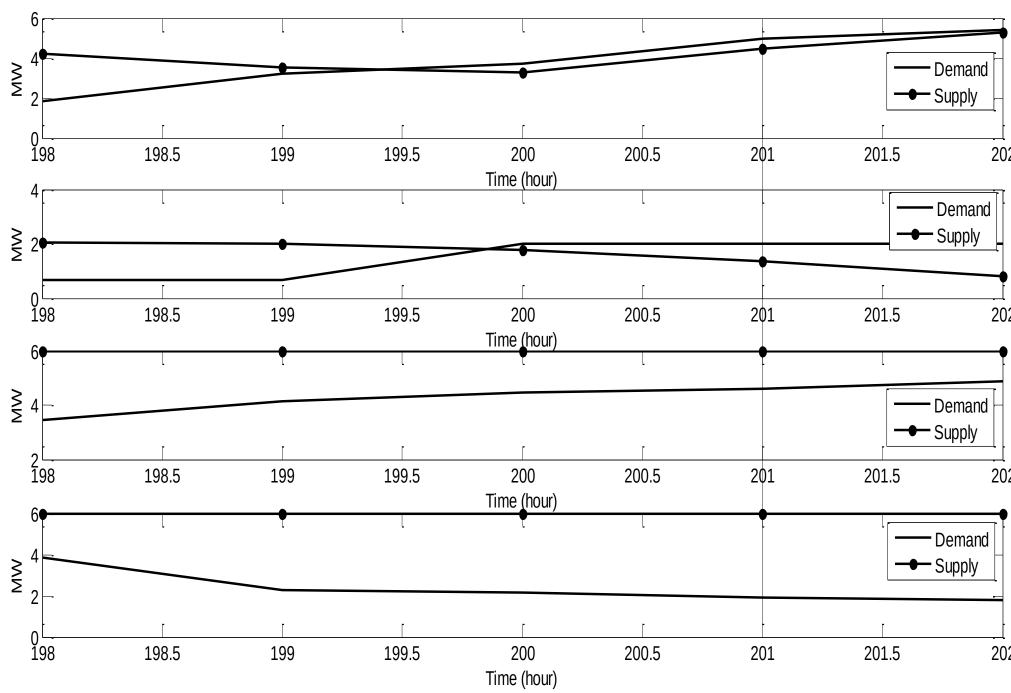

Fig.3.16 The total demand and supply in MG1, MG2, MG3 and MG4 respectively

Chapter 4

SIMULATION AND RESULTS

4.1. Introduction

The MG gets its power from two main renewable resources: the wind and solar. The capacity of the wind farm or the solar power in each section is 25 MW. The average load of the whole system is 12.3 MW and the peak load is 20 MW. One year load data have been selected for usage, and the simulation runs have been performed over 20 years period. The energy rating of ESS is 20 MWh and the power rating is 4 MW. The initial stored energy in the energy storage is assumed to be 100% of the energy capacity of the storage. The reliability data of energy storage are shown in Table 4.1, while Table 4.2 summarizes the reliability data of the wind turbines [76] and PV system [91].

Table 4.1 Data of Energy Storage System

Parameters of ESS	**Values**
Energy rating (MWh)	20
Power rating (MW)	10
Min SOC	50%
Max SOC	100%
Failure rate (f/year)	0.1
Repair rate (r/year)	0.3

Table 4.2 Data of WT, PV System

Parameters	**Wind Turbine**	**PV system**
Number	5	1
Capacity	10 MW	50 MW
Cut in speed	4 m/s	-
Rated speed	15 m/s	-
Cut out speed	26 m/s	-
Mean failure rate	1.8 f/year	0.6 f/year
Repair rate	0.2 r/year	0.2 r/year

The simulation has been performed under four different cases as illustrated in Table 4.3. In each case, the system simulates the RBTS data with the source power hour by hour and computes the reliability indices.

Table 4.3 Simulation Cases

Case	Energy storage	Uncertainty
Case 1	Excluded	Excluded
Case 2	Excluded	Included
Case 3	Included	Excluded
Case 4	Included	Included

The reliability data of the IEEE-RBTS system has been used in all the cases. These data are summarized in Table 4.4 and Table 4.5.

Table 4.4 Reliability Data of Transformers

Component	Failure Rate (f/y)	Repair Rate (r/y)	Replacing Rate (r/y)
Tr. 11/0.415 kv	0.015	43.8	876

Table 4.5 Reliability Data of the Distribution Lines in the RBTS System

Line number	Failure rate (f/y)	Repair rate (r/y)
2, 6, 10, 14, 17, 21, 25, 28, 30, 34	0.039	1752
1, 4, 7, 9, 12, 16, 19, 22, 24, 27, 29, 32, 35	0.04875	1752
3, 5, 8, 11, 13, 15, 18, 20, 23, 26, 31, 33, 36	0.052	1752

4.2. Simulation of Solar and Wind Power

4.2.1. Simulation of Solar Power

Fig. 4.1 shows the first 100 hours of the forecasted time series by the use of the three exponential smoothing models for a prediction horizon of one hour. Table 4.6 summarizes the results of the statistical coefficients for the three exponential models for prediction horizon of 1 hour. It can be seen that the coefficients confirm that triple exponential smoothing is the best model.

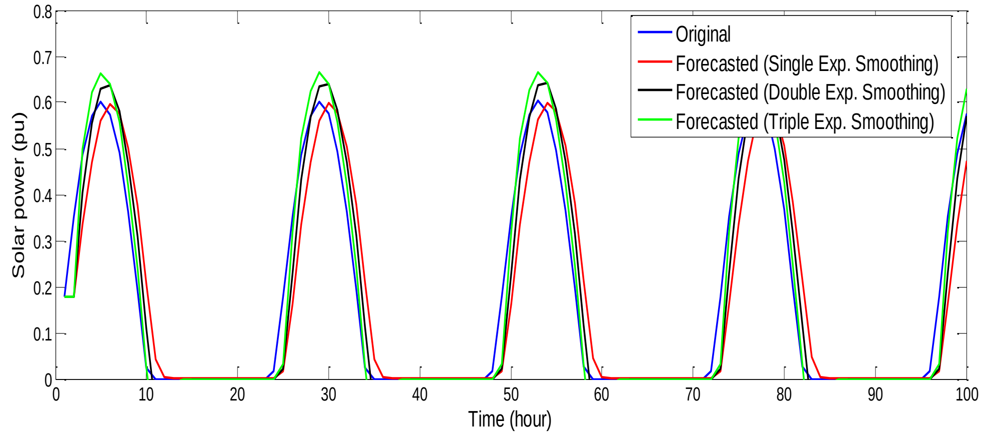

Fig.4.1 1st 100 hrs. From the Original and the Forecasted Time Series by the Three Exponential Smoothing Models, (Forecast horizon of 1 hrs.).

Table 4.6 Comparison of the Three Exponential Smoothing Models

Coefficient	Single smoothing	Double smoothing	Triple smoothing
$r_{x\hat{x}}$	0.9278	0.9815	0.9939
RMSE	0.1270	0.0687	0.0482
MAE	0.0863	0.0439	0.0300
MAPE	0.3155	0.1603	0.1095

Fig. 4.2 shows the entire original time series and the forecasted time series by the use of triple exponential smoothing model for a horizon of one hour. The forecast of solar power is used to give a perspective about the solar power values.

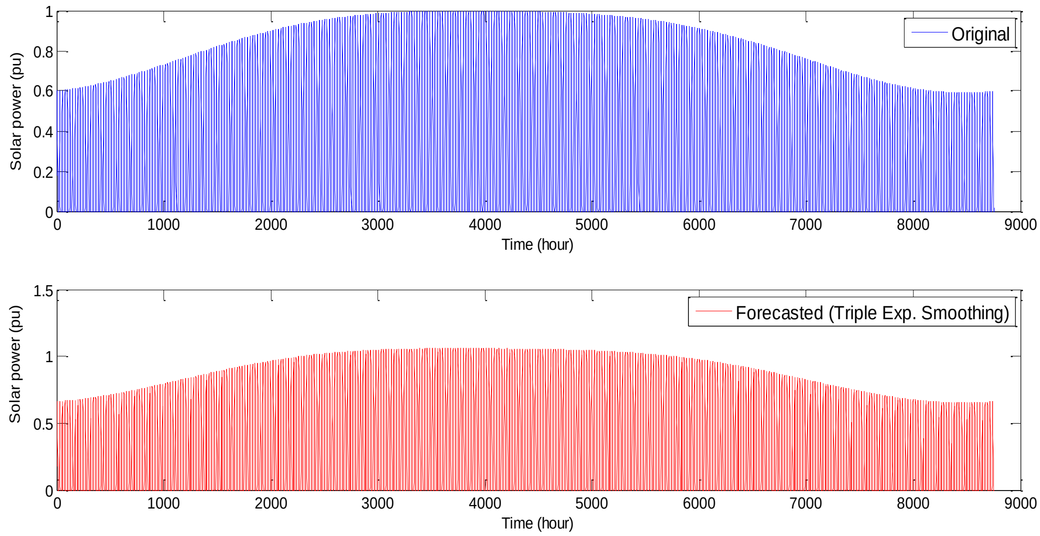

Fig.4.2 The original and the forecasted time series by triple exponential smoothing model. Forecast horizon of 1 hr.

The assessment results of aforementioned statistical coefficients for the triple exponential smoothing are summarized in Table 4.7. This table has been achieved from forecasting results for prediction horizons of 1, 2 and 3 hours. It is noted from Table 4.7, when the horizon of prediction increases, all indexes get worse. This shows that long-term forecasting of solar power cannot be accomplished by the triple exponential smoothing because of the error introduced with longer time steps.

Table 4.7 Model Assessment Triple Exponential Smoothing

Forecasting Horizon	1 hr.	2 hr.	3 hr.
$r_{x\hat{x}}$	0.9939	0.9397	0.7947
RMSE	0.0482	0.1558	0.2916
MAE	0.0300	0.1033	0.1973
MAPE	0.1095	0.3777	0.7214

The forecasting horizon of 1 hour, 2 hours and 3 hours for 100 hours period are shown in Fig. 4.3. As shown in Fig. 4.3, these curves certify the noted remark in table 4.7, the accuracy decreases as the forecasting horizon increases. The reason in that the solar power data has nonlinear and time-varying nature due to the meteorological conditions and night time, which increases the complexity in predicting its values in the long-term predictions. The solution for this problem is by using the historical data and physical data such as the humidity, temperature distributions, the percentage of cloud in the sky across the year…

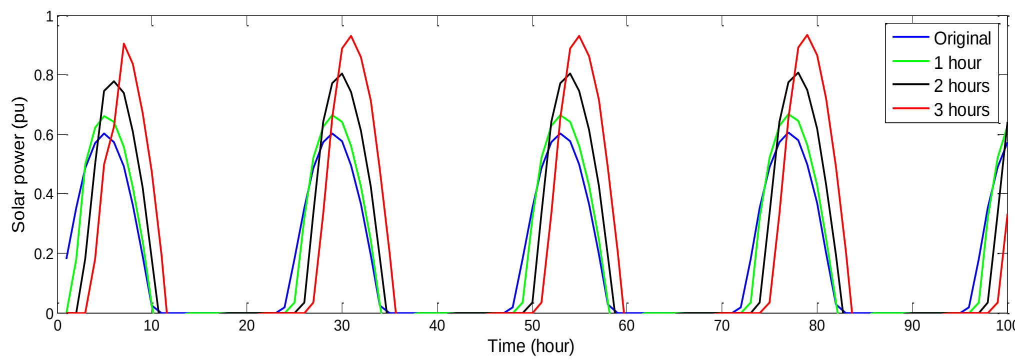

Fig.4.3 1st 100 hrs. from the original and the forecasted time series by triple exponential smoothing model, (Forecast horizon of 1, 2 and 3 hrs.).

4.2.2. Simulation of Wind Power

In this thesis, ARMA method is selected to model the wind speed data. When ARMA is used, first step is to decide which ARMA model that best fits the time-series behavior. Therefore, the autocorrelation and partial autocorrelation functions are used and plotted in Fig. 4.6. The wind speed data in this thesis is a 6 years historical wind speed from [70].

The autocorrelation coefficient in Fig. 4.4 decreases slowly when the time-lag increases. It indicates that an autoregressive model may fit the time series. The partial autocorrelation graph confirms that the autoregressive model will best fit the time series. Because the partial autocorrelation starts decay from the second lag, it establishes an autoregressive model of order 2, ARMA(2,0).

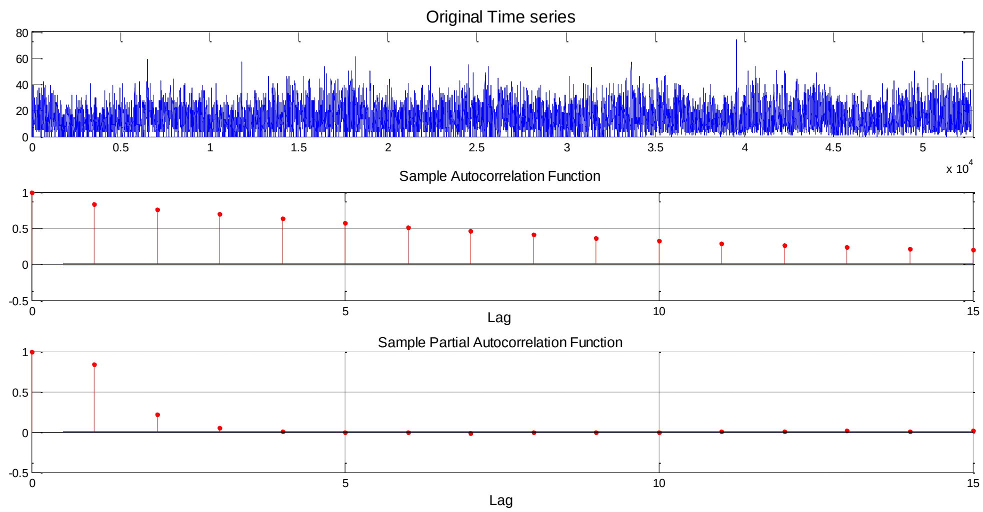

Fig.4.4 Original time series, and the autocorrelation functions

Fig. 4.5 shows the autocorrelation and partial autocorrelation coefficients of the first-derivative time-series. The autocorrelation graph confirms that the autoregressive integrated moving average ARIMA (0,1,1) model is possible, since the autocorrelation function begins decaying from the first time lag.

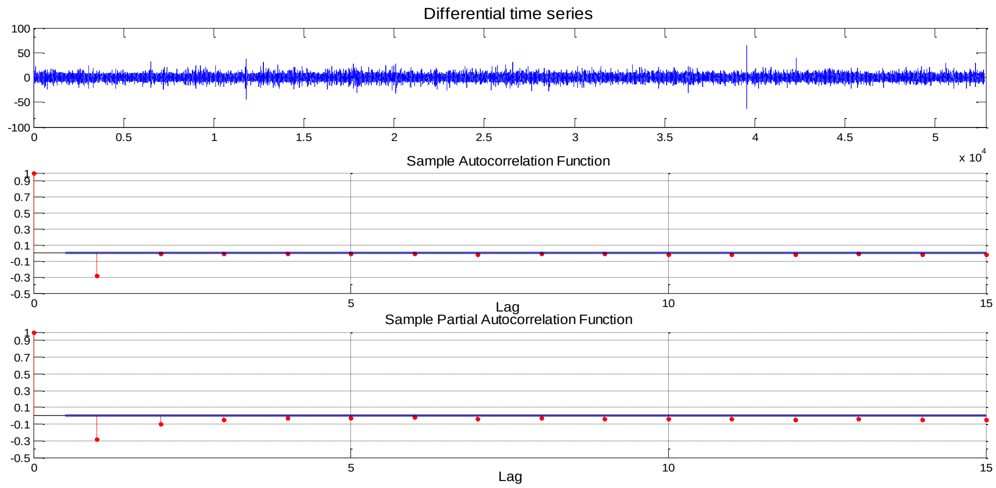

Fig.4.5 Differential time series, and the autocorrelation functions

Fig. 4.6 shows the autocorrelation and partial autocorrelation coefficients of the second-derivative time-series. As it can be seen, an autoregressive integrated moving average (0,2,2) model is possible, because the autocorrelation graph decays from the second lag.

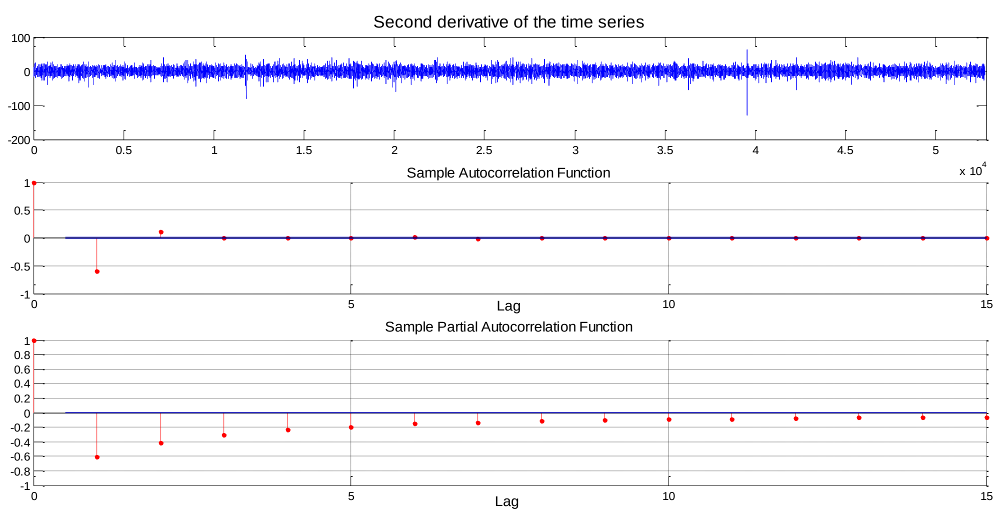

Fig.4.6 Second-derivative time series, and the autocorrelation functions

Since ARIMA (2,0,0) is the model that is purely regressive of order 2 and does not involves integration, this results in the least time-consuming model and the easiest to implement. Therefore, ARIMA (2,0,0) is selected as the forecasting model for the wind speed. The values of the autoregressive coefficients are 0.656687 and 0.213976. The constant term value is 1.85267. The error variance is 0.0698.

Fig. 4.7 shows the first 100 hours of the forecasted time series by using the ARIMA(2,0,0) model for a prediction horizon of one hour. Fig. 4.8 shows the entire forecasted time series using the ARIMA(2,0,0) model for a horizon of 1 hour.

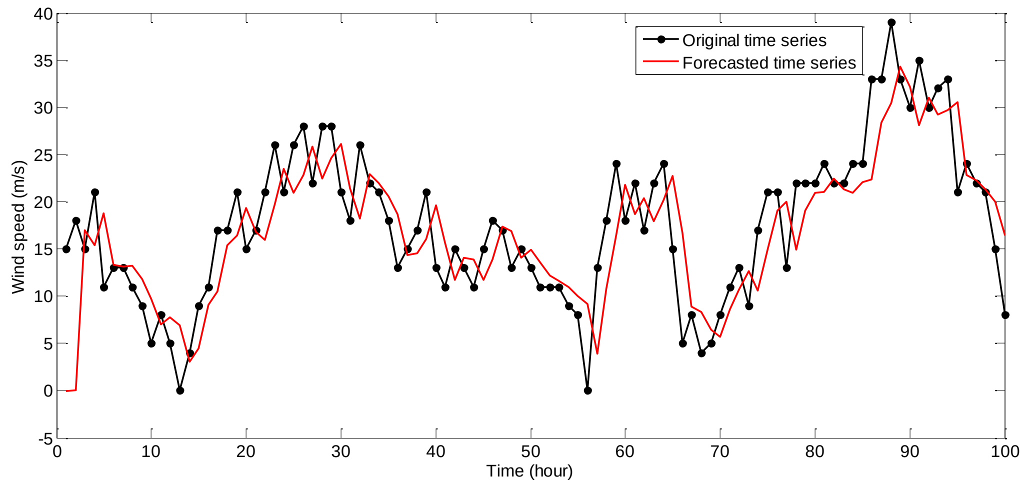

Fig.4.7 1st 100 hrs. from the forecasted and the time original series by ARIMA (2,0,0), forecast horizon of 1 hr.

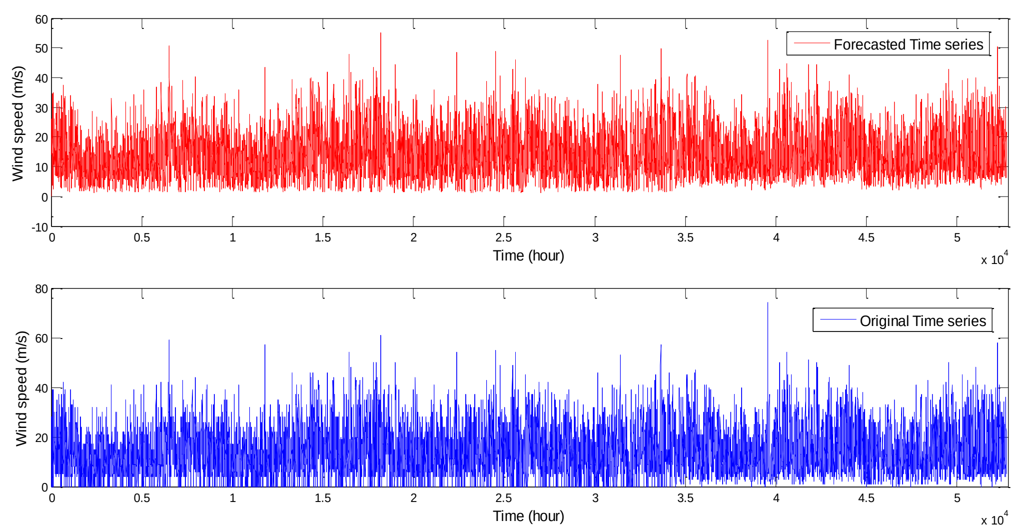

Fig.4.8 The forecasted and the original time series by ARIMA (2,0,0), forecast horizon of 1 hr.

The assessment results of these coefficients for the ARIMA (2,0,0) are summarized in Table 4.8. This table has been produced from the results of prediction horizons of 1, 2 and 3 hours. It is noted from table 4.8, when the prediction horizon increases, all quality indexes get worse. The forecasting horizon of 1 hour, 2 hours and 4 hours for 100 hours period are shown in Fig. 4.9.

Table 4.8 Model Assessment of ARIMA (2,0,0)

Forecasting Horizon	1 hr.	2 hr.	3 hr.
$r_{x\hat{x}}$	0.8432	0.7688	0.6989
RMSE	4.2490	5.0839	5.7668
MAE	3.1878	3.8274	4.3438
MAPE	0.2224	0.2670	0.3033

These curves also confirm that the ARIMA(2,0,0) model is invalid for long term forecasting. The reason in that the wind speed time series becomes non-stationary stochastic process in long-term prediction because of the strong impact of the meteorological conditions on the wind speed and the weak correlation between wind speeds in the long-term forecasting.

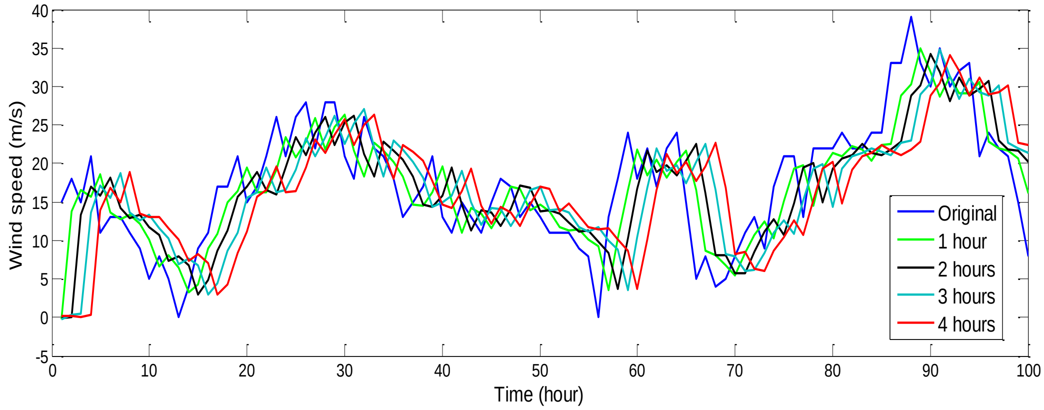

Fig.4.9 1st 100 hrs. from the forecasted and the original time series by ARIMA (2,0,0). Forecast horizon of 1, 2, 3 and 4 hrs.

4.3. Impacts of Wind, Solar and Energy Storage on the Reliability of Microgrid

4.3.1. Impact of Wind Power Capacity

In this case, the energy storage is set to 20 MWh. The power rating of the energy storage is set to 5 MW. This case also incorporates the uncertainty in wind speed by using the mean absolute percentage error (MAPE). The MAPE of wind speed has been found 0.2225 for 1 hour prediction horizon.

In order to better understand the wind power capacity impact on microgrid reliability, the wind capacity increases from 5 to 25 MW in this case. Correspondingly, Figs. 4.10 and 4.11 show the impact of wind power capacity on EENS and EENU. As seen, large wind power capacity will reduce EENS and increase EENU in RBTS at fixed capacity of energy storage. In addition, these figures show that using energy storage will reduce the EENS and EENU with large amount.

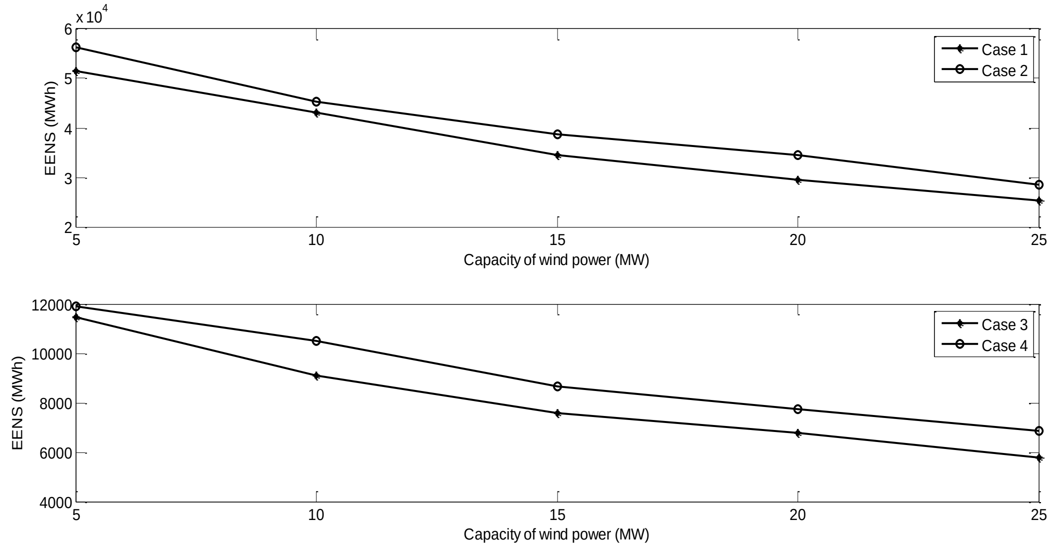

Fig.4.10 Impact of wind power capacity on EENS

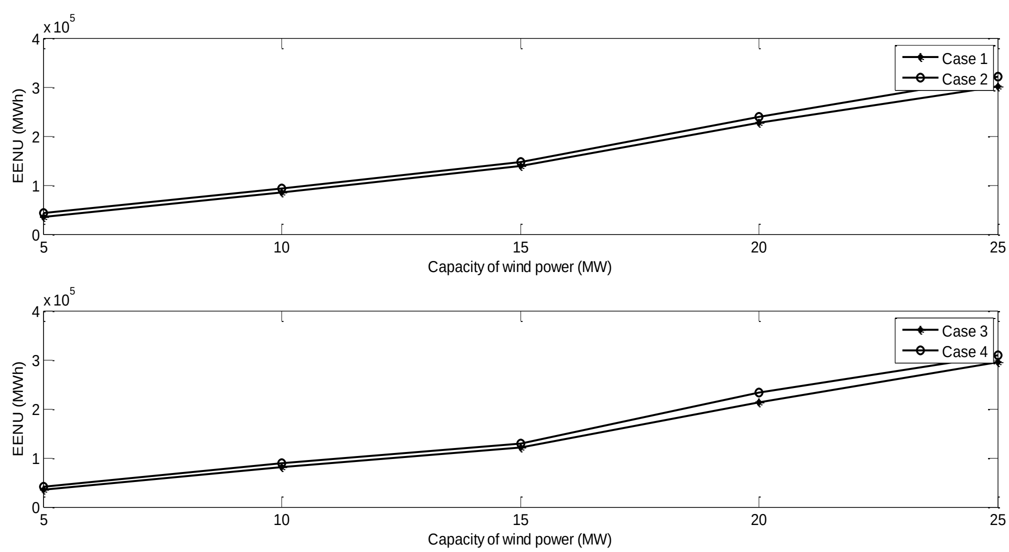

Fig.4.11 Impact of wind power capacity on EENU

The impact of wind power capacity on SAIDI and SAIFI is shown in Figs. 4.12 and 4.13, respectively. As seen, large wind power capacity will decrease SAIDI and SAIFI in RBTS at large wind power capacity with fixed energy storage. Figs. 4.12 and 4.13 show that the uncertainty in wind speed has large impact at small wind power capacity while this impact decreases as wind power capacity increases.

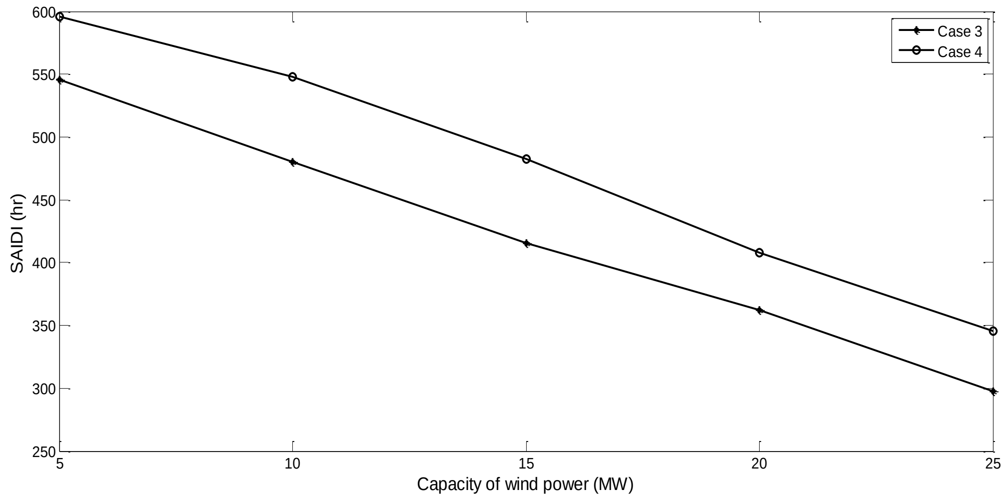

Fig.4.12 Impact of wind power capacity on SAIDI

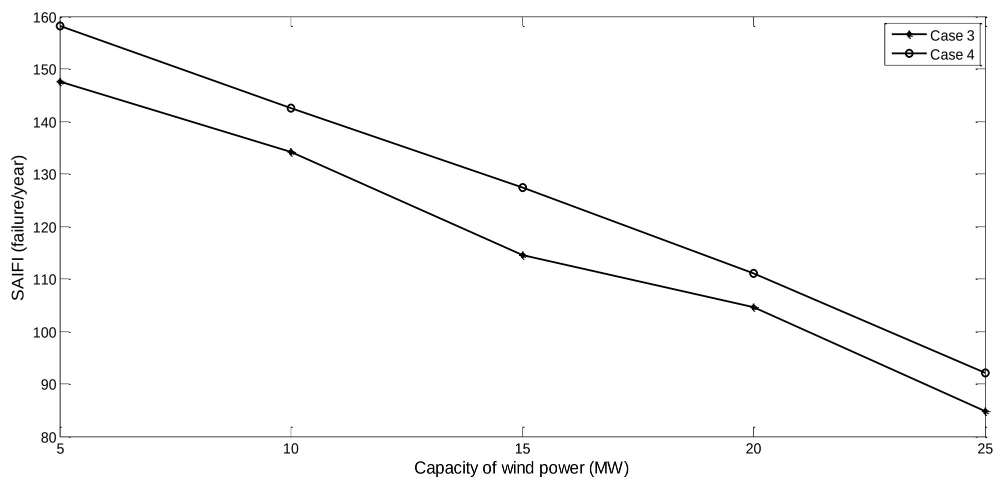

Fig.4.13 Impact of wind power capacity on SAIFI

4.3.2. Impact of Solar Power Capacity

The impact of the solar power capacity on system reliability is explained in this case. The MAPE of the solar power has been found 0.1095 for the 1 hour prediction horizon. When the solar power capacity increases from 5 MW to 25 MW, the corresponding EENS and

EENU are shown in Figs. (4.14- 4.15). EENS does not decrease much as the solar power capacity increases. When energy storage is used, large solar power capacity will reduce EENS at fixed capacity of energy storage. Also, it can be noted that the values of EENS and EENU drops when energy storage is used compared to the case when energy storage is not used. The key role of energy storage in improving system reliability is the ability of energy storage in transferring excess solar energy from one time step to others.

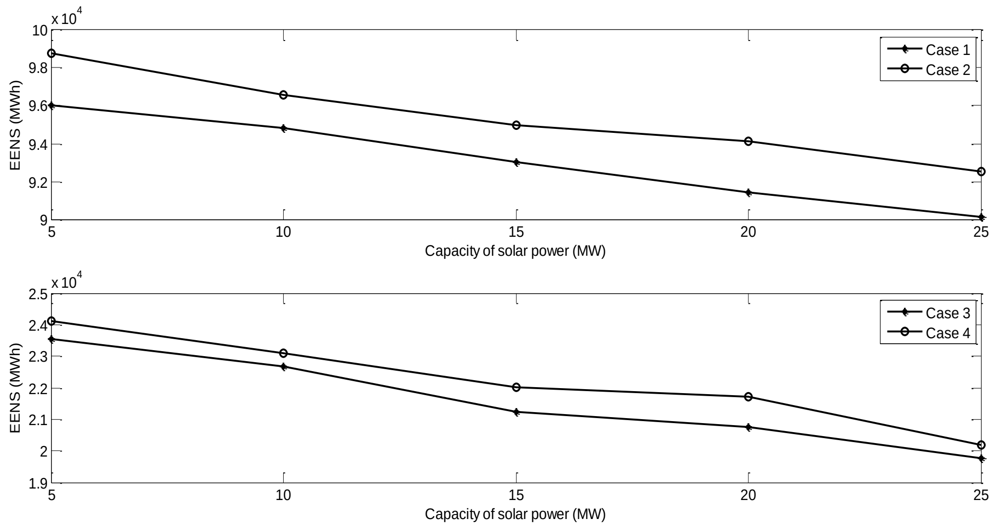

Fig.4.14 Impact of solar power capacity on EENS

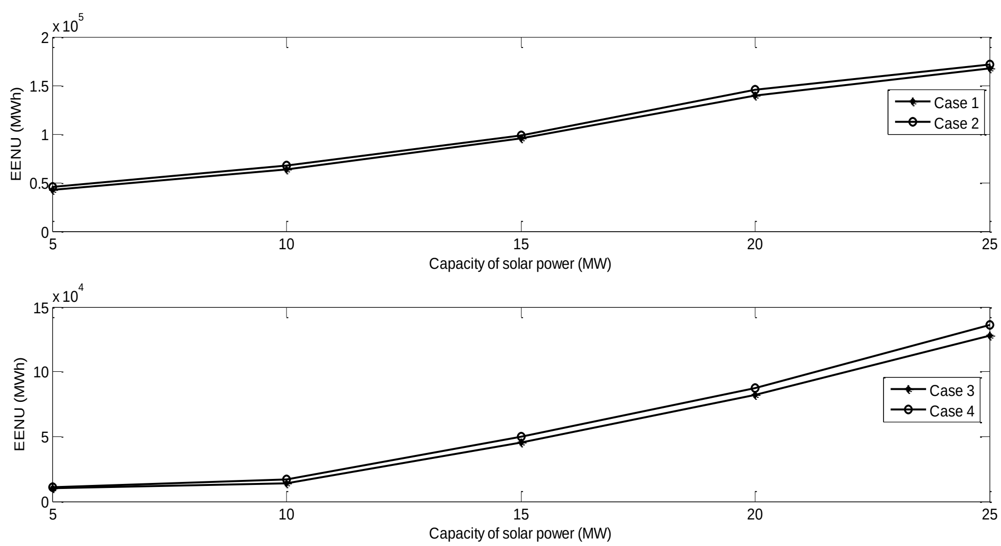

Fig.4.15 Impact of solar power capacity on EENU

The impact of solar power capacity on SAIDI and SAIFI is shown in Figs. 4.16 and 4.17, respectively. As seen, SAIDI and SAIFI do not decrease much in IEEE-RBTS at large solar power capacity with fixed energy storage. This is due to the huge number of hours that solar power is not available which requires energy storage with large energy rating.

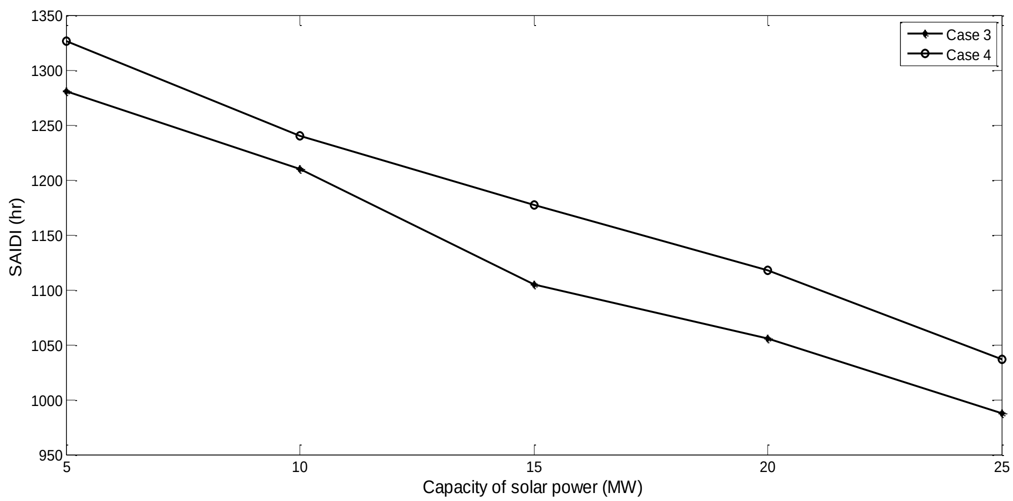

Fig.4.16 Impact of solar power capacity on SAIDI

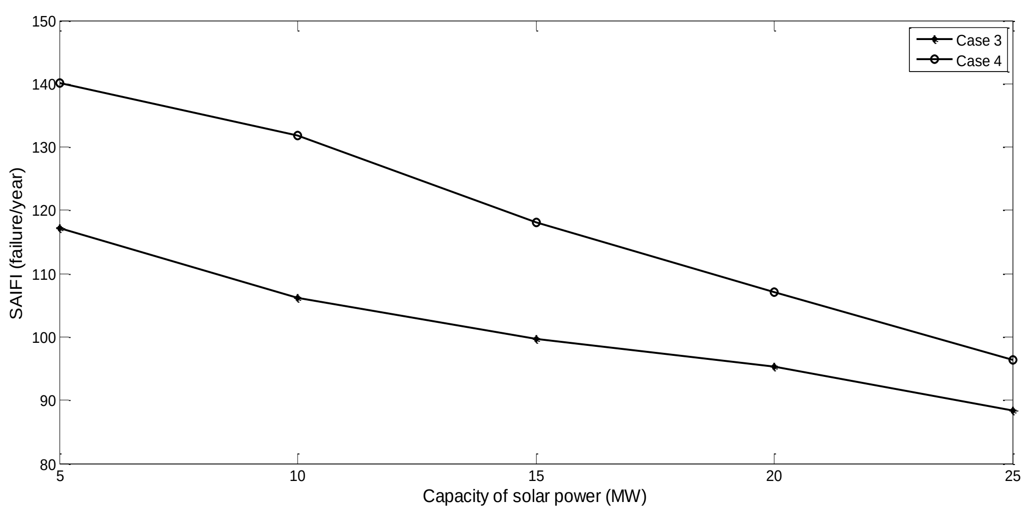

Fig.4.17 Impact of solar power capacity on SAIFI

4.3.3. Impact of Hybrid Wind-Solar Power Capacity

This case explains the impact of hybrid wind-solar power capacity on microgrid reliability. Capacity of every power plant is the half of the installed capacity. Hence, each power plant capacity increases from 2.5 MW to 12.5 MW. Correspondingly, Figs. 4.18 and 4.19 show the impact of hybrid wind-solar power capacity on EENS and EENU. It is clear that large hybrid wind-solar power capacity will reduce EENS and increase EENU in RBTS at fixed capacity of energy storage. In addition, these figures show that using energy storage will reduce the EENS and EENU with large amount. It can be noted that the solar and wind power shared in reducing the EENS at low wind power capacities although the solar power can't reduce the EENS. This is due to the complementary features of the sun and wind that reduce the probability of both power plants cannot produce power at same time.

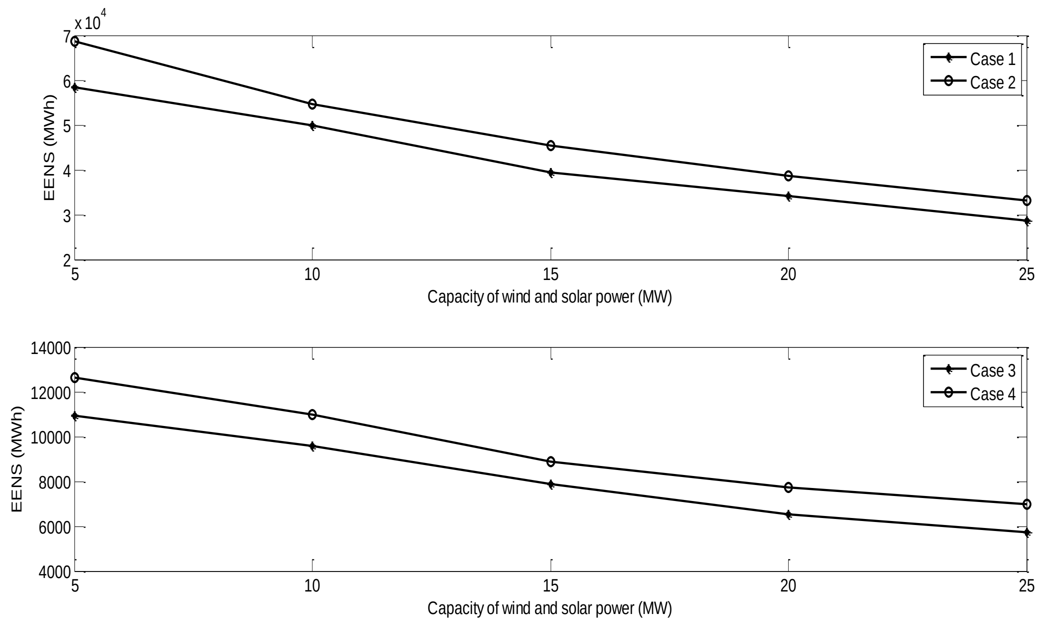

Fig.4.18 Impact of wind and solar power capacity on EENS

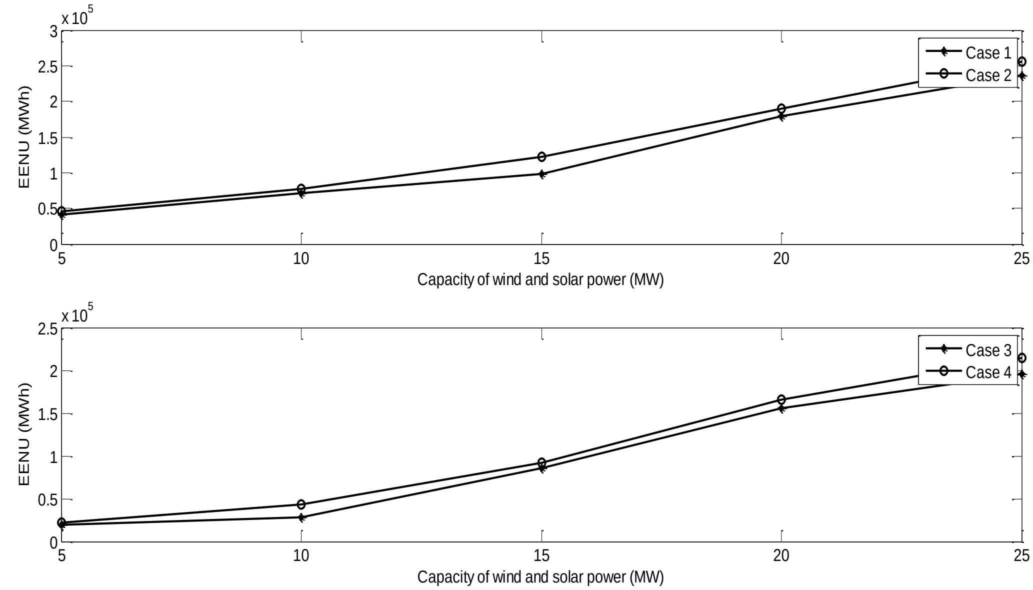

Fig.4.19 Impact of wind and solar power capacity on EENU

The impact of wind and solar power capacities on SAIDI and SAIFI is shown in Figs. 4.20 and 4.21, respectively. As seen, large power capacity will decrease SAIDI and SAIFI at large power capacity with fixed energy storage but their values are still large. Figs. 4.20 and 4.21 show that the uncertainties in wind speed and solar power have large impact at small power capacities while this impact decreases as power capacity increases.

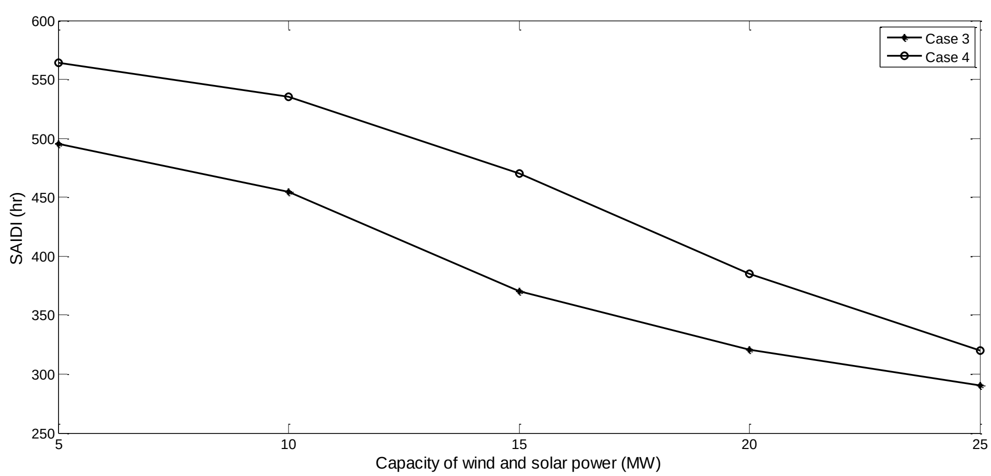

Fig.4.20 Impact of wind and solar power capacity on SAIDI

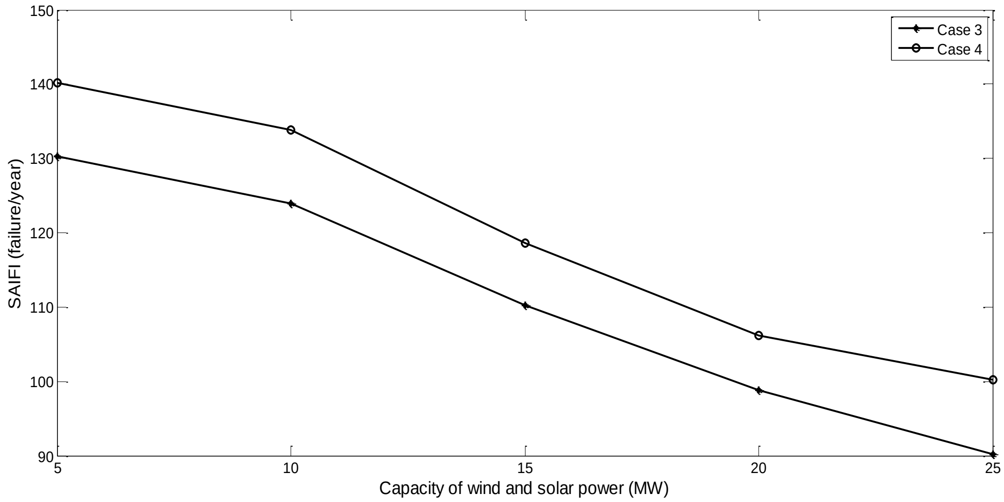

Fig.4.21 Impact of wind and solar power capacity on SAIFI

4.4. Impact of the Smart Restoration on the Microgrid Reliability

This case studies the impact of the smart restoration on the reliability of the stand-alone MG system when wind or solar energy or both are used as the main energy supply system. The interrupted load points are recovered from a failure state by using the stored energy or the excess energy from the neighbors. The load priority and optimal operation sequence are assumed separately in each MG to restore the load. RBTS bus 2 can be viewed as ring topology with multiple power sources after using the smart restoration as shown in Fig. 3.15. The MGs are connected to each other through switches and the common bus. When there is a power shortage in the MG, the smart restoration looks for energy storage or another path to restore the load point. If a load point is isolated from the grid by a failure, the load point will experience a permanent failure unless there is distributed storage near the load point. The imported power from the neighbors can pass through the switches on the ring path or by the common bus.

The simulation in this section has been done under four cases as explained in the following table.

Table 4.9 Simulation Cases of the Smart Restoration

Case	Energy Storage	Smart Restoration	Uncertainty
Case 1	Included	Excluded	Included
Case 2	Included	Included	Included
Case 3	Excluded	Excluded	Included
Case 4	Excluded	Included	Included

4.4.1. Scheduling Resources in Smart Restoration

Fig. 4.22 shows the total demand and supply in the MG1, MG2, MG3 and MG4, respectively. Fig. 4.23 shows 6 hours of the dispatchable generator and energy storage operations. At hour 198, the total supply exceeded the total demands. Therefore, the energy storage was charged while it was discharged in the next hours.. At hour 201, the energy storage and the supply are not enough to match the demand. Therefore, dispatchable generator, with ramping rate 4 MW and capacity 8 MW, started at this hour.

From Fig. 4.22 and 4.23, it can be seen that smart restoration played a key role, where it operated the dispatchable generator at hour 201 at rate 4 MW and discharged the energy storage at rate of 3 MW to cover the shortage instead of discharging the energy storage at rate 5 MW and operating the generator at rate 2 MW.

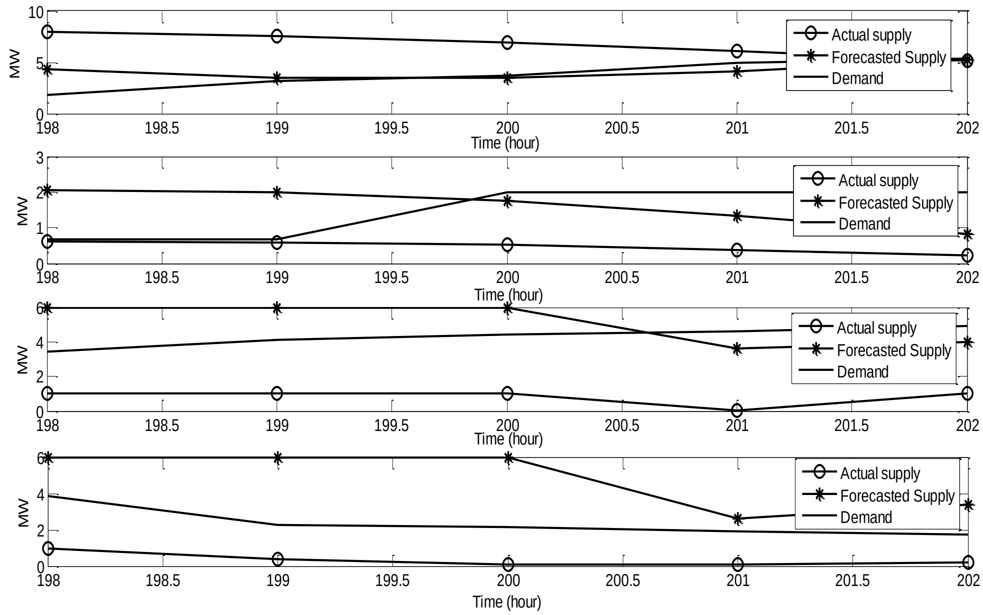

Fig.4.22 Total demand and supply in MG1, MG2, MG3 and MG4 before using smart restoration

The smart restoration used the forecasted supply to determine the best plan to operate the generator and energy storage based on the look-ahead capability. Therefore, it operated the generator at its max ramping up (4 MW) to cover the shortage in the next hours that requires the total capacity of the generator.

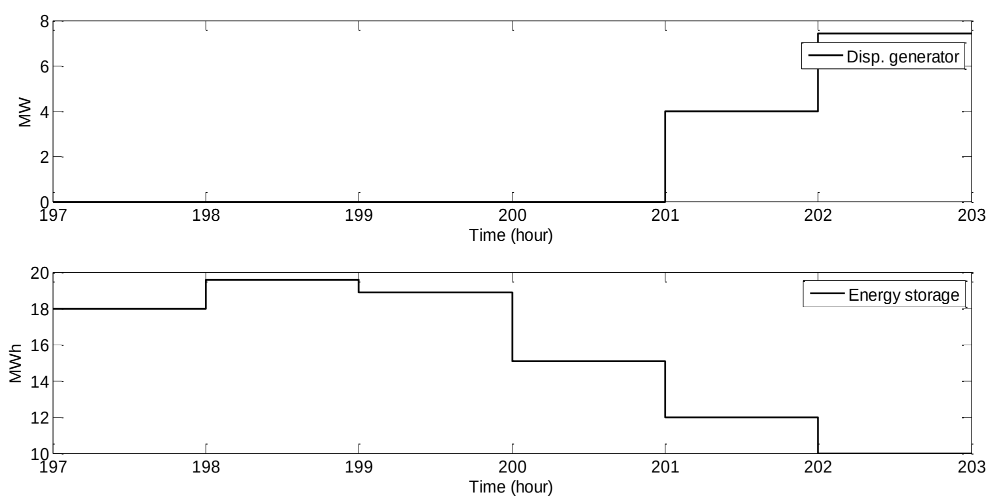

Fig.4.23 Operation of dispatchable generator and energy storage

Fig. 4.24 shows the total demand and supply in the four MGs after using smart restoration. It can be seen that the supply matches the demand at every point of time.

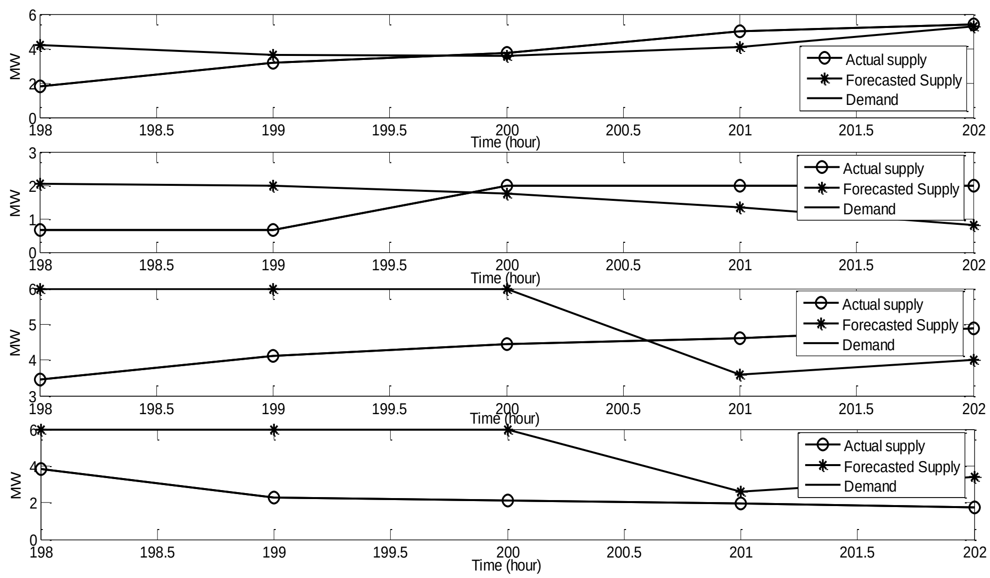

Fig.4.24 Total load and demand in MG1, MG2, MG3 and MG4 after using smart restoration

4.4.2. The Smart Restoration with Wind Energy

In this case the smart restoration is applied to MG. The energy storage capacity is set to 20 MWh. As well as the capacity of the wind power is increasing from 5 MW to 25 MW to assess the suitable wind power capacity. Correspondingly, Figs. (4.25-4.26) show the impact of the smart restoration on EENS and EENU. Fig. 4.25 compares EENS when there is no energy storage and when the energy storage is used. The smart restoration is more able to reduce the EENS at small wind power capacity than at large wind power capacity. When the wind power capacity is large with respect to the load, the probability of the excess wind energy increases in the neighbors in which the smart restoration can use it to restore the load points that are in down state.

Fig. 4.26 shows that using of the smart restoration will decrease the ENU but not much, the difference is not clear because the range of EENU is large.

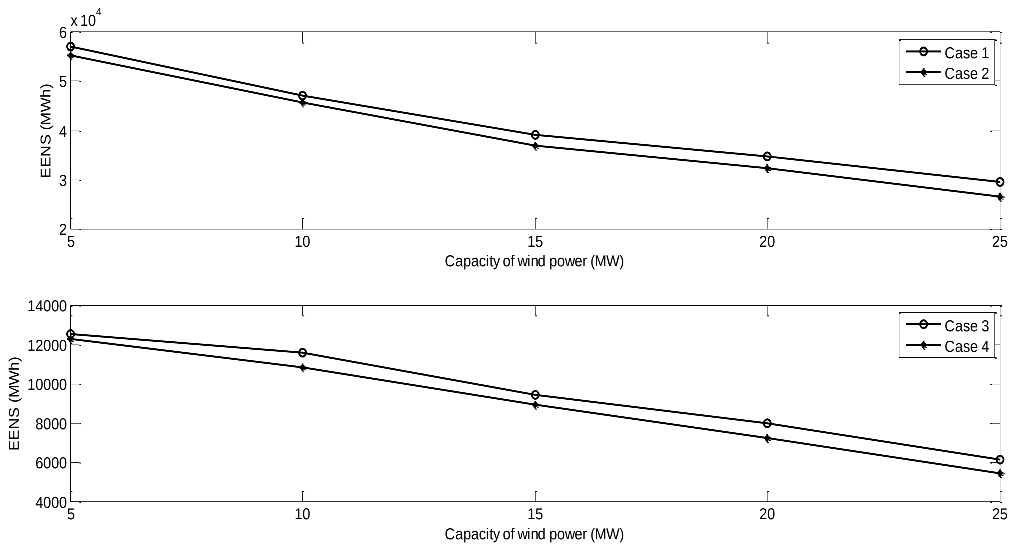

Fig.4.25 Impact of smart restoration on EENS

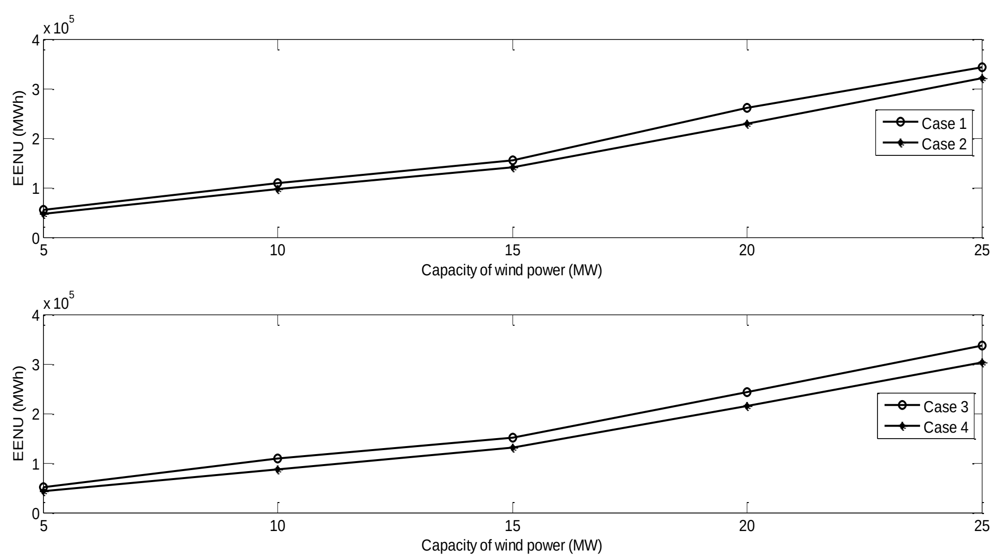

Fig.4.26 Impact of smart restoration on EENU

The impact of the smart restoration on SADI and SAIFI are shown in Figs. (4.27-4.28). Fig. 4.27 shows that the smart restoration will not significantly reduce the SAIDI at small wind power capacity but it does at large wind power capacity. When wind power capacity is large with respect to the load, the probability of the excess wind energy increases in the neighbors in which the smart restoration can use it to restore the load points that are in down state.

Using of the smart restoration at wind power capacity 25 MW reduces SAIDI by 20 hrs. Fig. 4.28 also shows that the smart restoration will not significantly reduce the SAIFI at small wind power capacity but it will do at large wind power capacity. Using of the smart restoration at wind power capacity 25 MW reduces SAIFI by 5 failures/year.

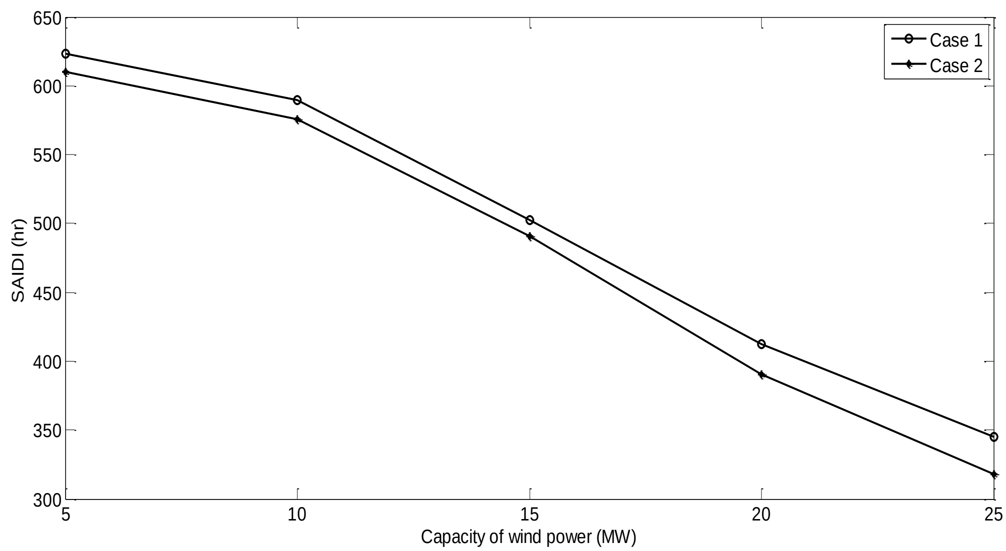

Fig.4.27 Impact of smart restoration on SAIDI

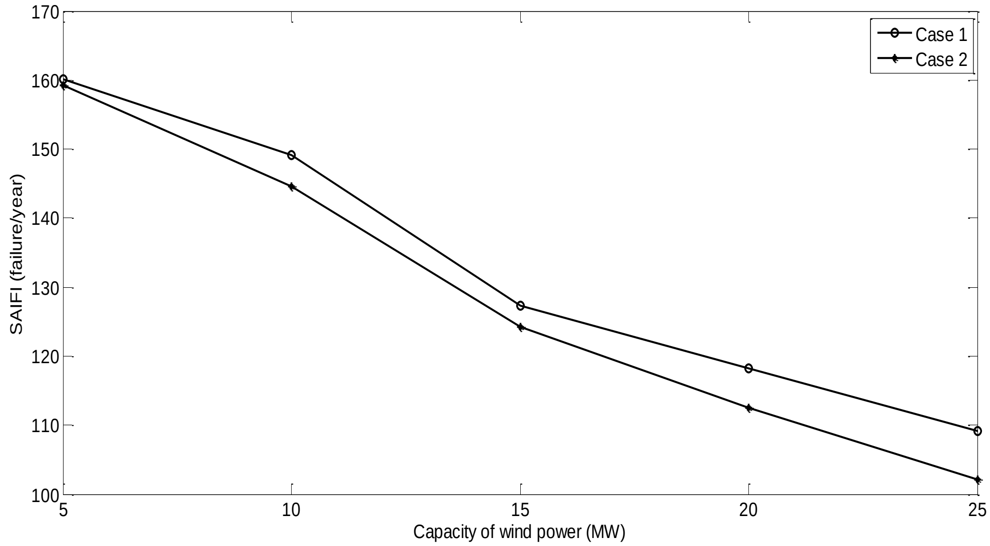

Fig.4.28 Impact of smart restoration on SAIFI

4.4.3. The Smart Restoration with Solar Energy

The capacity of the solar power is increasing from 5 MW to 25 MW to assess the suitable solar power capacity. Figs. (4.29-4.30) show the impact of the smart restoration on EENS and EENU. Fig. 4.29 shows EENS when there is no energy storage, and when the energy storage is used. It can be seen from the two figures that the smart restoration will not also significantly reduce the EENS at small solar power capacity but it will do at large solar power capacity. Again, when the solar power capacity is large with respect to the load, the probability of the excess solar energy increases in the neighbors in which the smart restoration can use it to restore the load points that are in down state.

Fig. 4.30 shows that using of the smart restoration will not decrease the ENU much. The reason of that, the sunlight is usually the same at all near regions as the case of the MG, and the sun does not shine at night, which makes solar energy is not available at all.

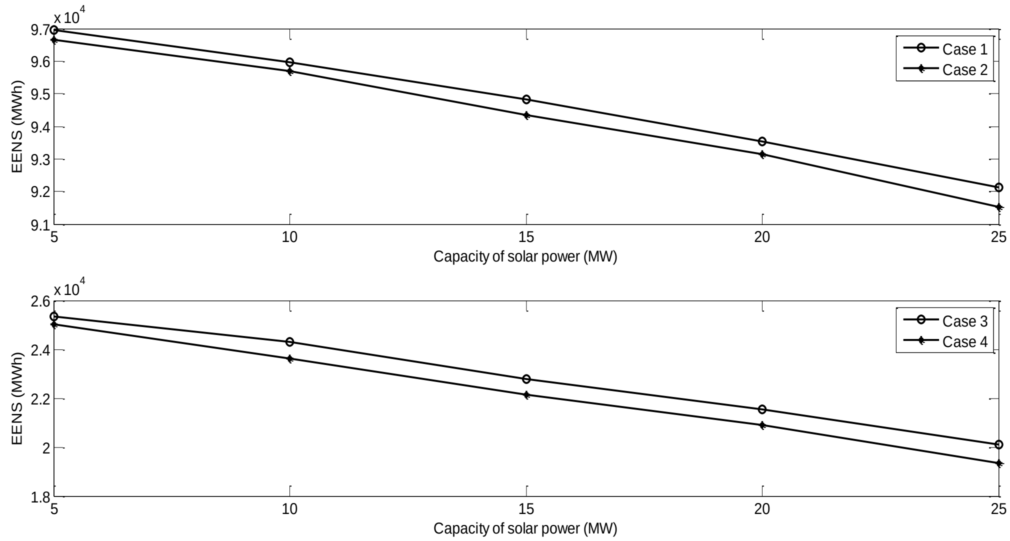

Fig.4.29 Impact of smart restoration on EENS

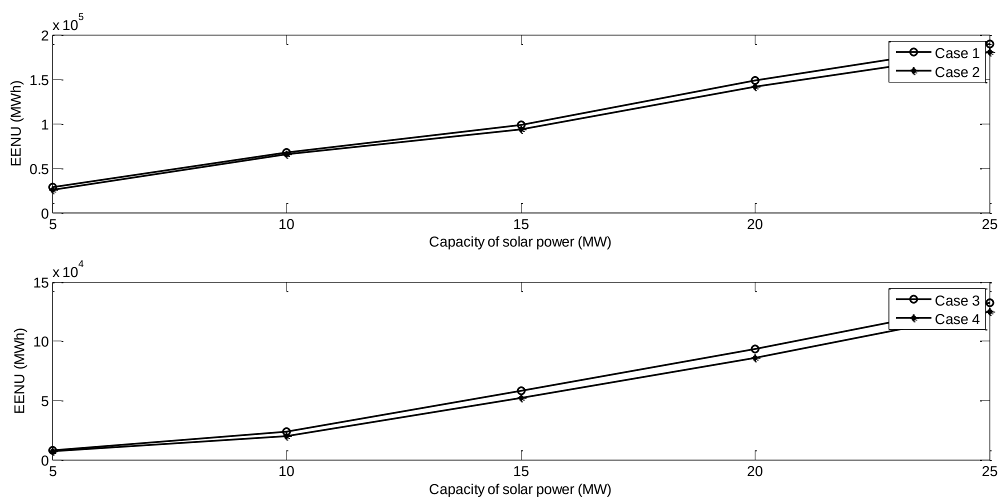

Fig.4.30 Impact of smart restoration on EENU

The impact of the smart restoration on SADI and SAIFI are shown in Figs. (4.31-4.32). Fig. 4.31 shows that the smart restoration will not significantly reduce SAIDI whatever the solar power capacity is. Fig. 4.32 shows that the smart restoration will not also significantly reduce the SAIFI at small and large solar power capacity. As mentioned before, the sunlight is usually the same at all near regions as the case of the MG and the sun does not shine at night in all regions which makes solar energy is not available at all. In other word, all MGs will face unavailability of the solar power at same time as well as it will face excess solar energy also at same time.

Using of the smart restoration with the solar energy will not decrease SAIDI significantly. Also, using of the smart restoration with the solar energy will not decrease SAIFI without using of the dispatchable generator.

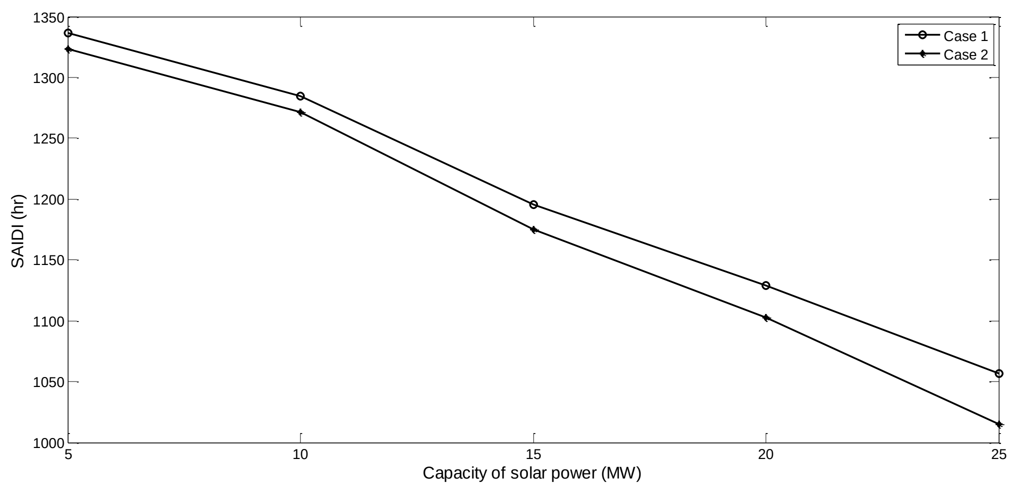

Fig.4.31 Impact of smart restoration on SAIDI

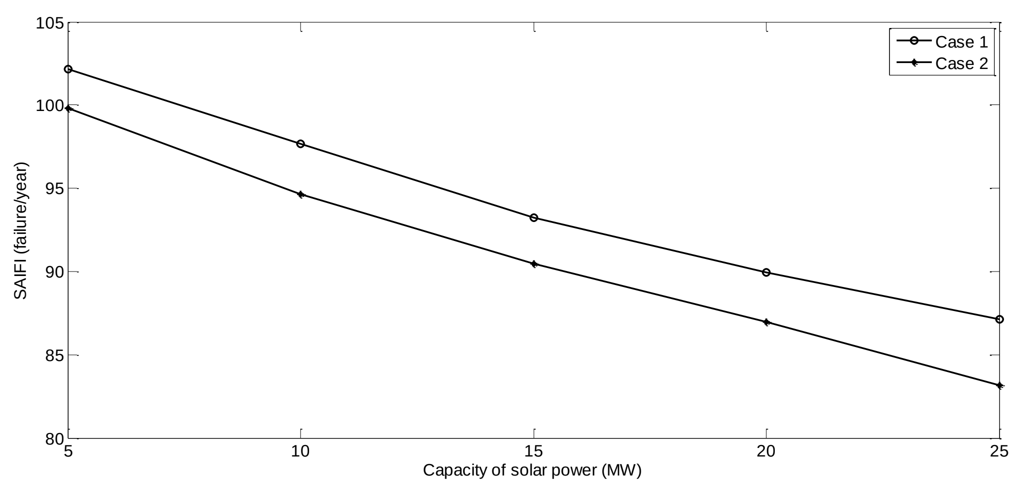

Fig.4.32 Impact of smart restoration on SAIFI

4.4.4. The Smart Restoration with Wind and Solar Energy

The capacities of the solar power and the wind power are increasing from 2.5 MW to 12.5 MW to assess the suitable wind and solar power capacities. In addition, the ISE level is set to 100% and the energy storage capacity is set to 20 MWh. Figs. (4.33-4.34) show the impact of the smart restoration on EENS and EENU. Fig. 4.33 shows EENS when there is no energy storage, and when the energy storage is used. It can be seen from the two figures that the smart restoration does not significantly reduce the EENS at small power capacity but it does at large power capacity. When the power capacity is large with respect to the load, the probability of the excess renewable energy increases in the neighbors in which the smart restoration can use it to restore the load points that are in down state.

Fig. 4.34 shows that using of the smart restoration will not significantly decrease the EENU due to the same reasons mentioned in solar energy case. In addition, the wind energy in this case is less than its size in the wind energy case.

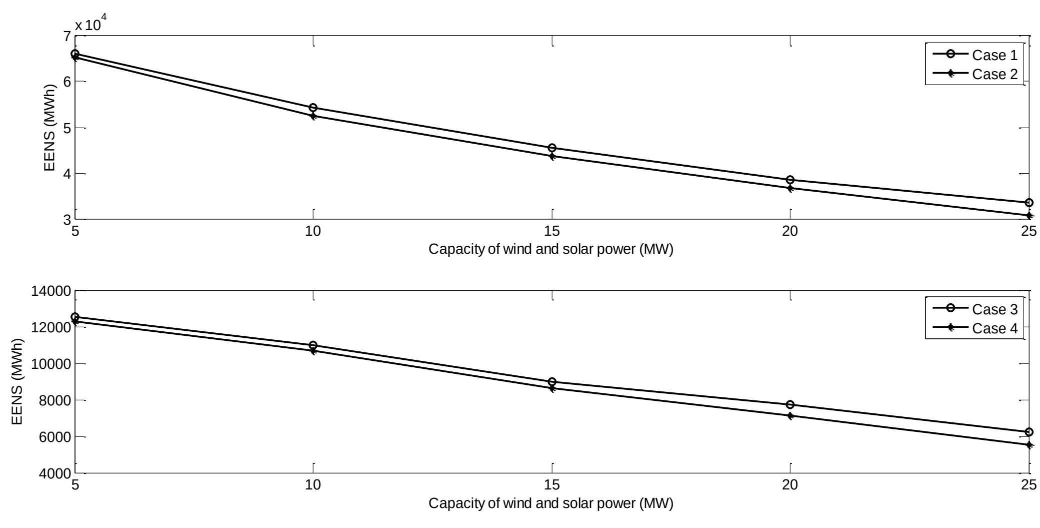

Fig.4.33 Impact of smart restoration on EENS

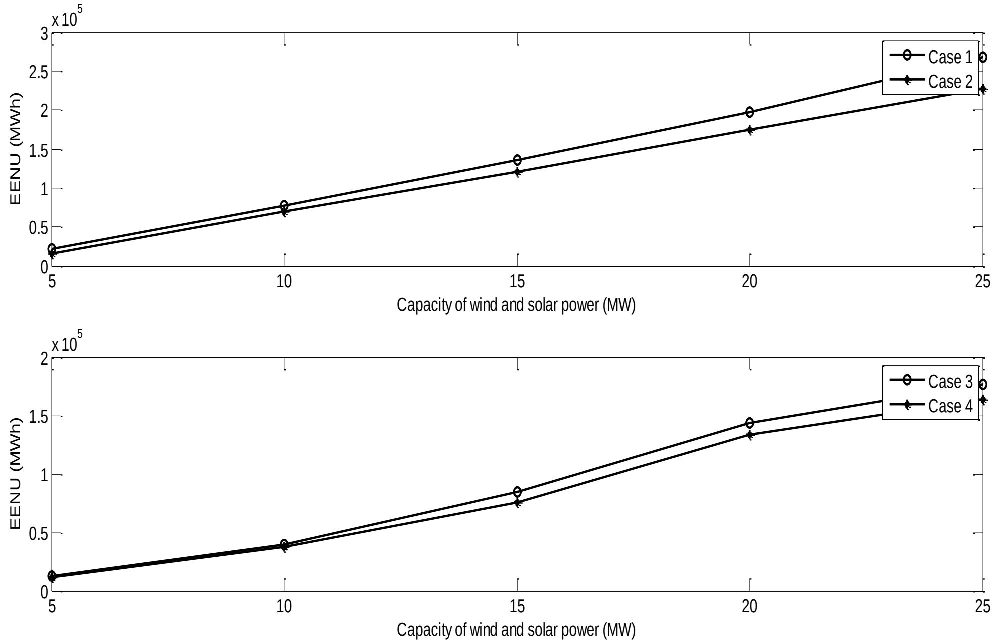

Fig.4.34 Impact of smart restoration on EENU

The impact of the smart restoration on SADI and SAIFI are shown in Figs. (4.35-4.36). Fig. 4.35 shows that the smart restoration will not significantly reduce the SAIDI or SAIFI at small power capacity but it will do at large power capacity. When power capacity is large with respect to the load, the probability of the excess renewable energy increases in the neighbors in which the smart restoration can use it to restore the load points that are in down state.

Fig. 4.36 also shows that the smart restoration will not significantly reduce the SAIFI at small power capacity but it will do at large power capacity.

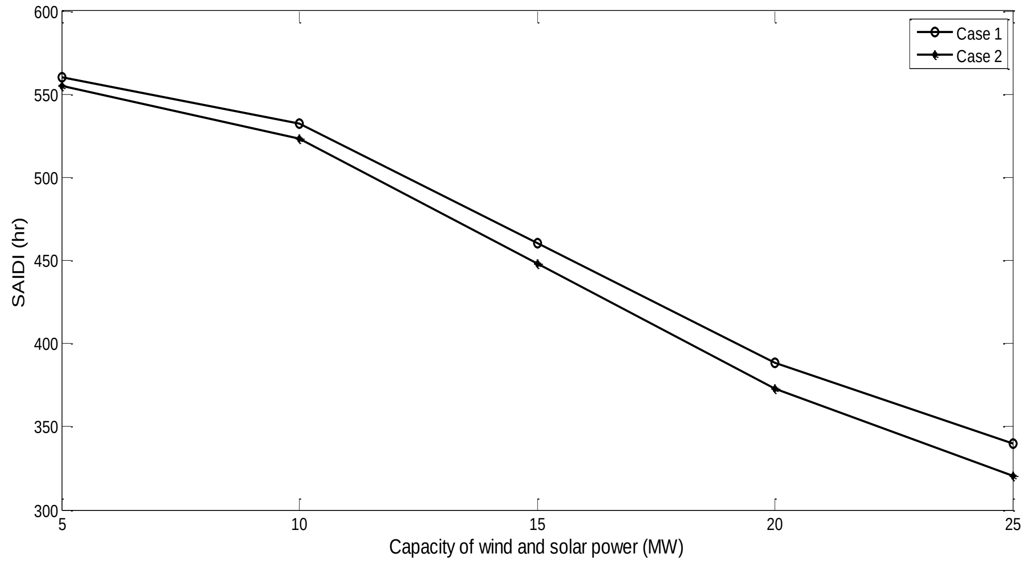

Fig.4.35 Impact of smart restoration on SAIDI

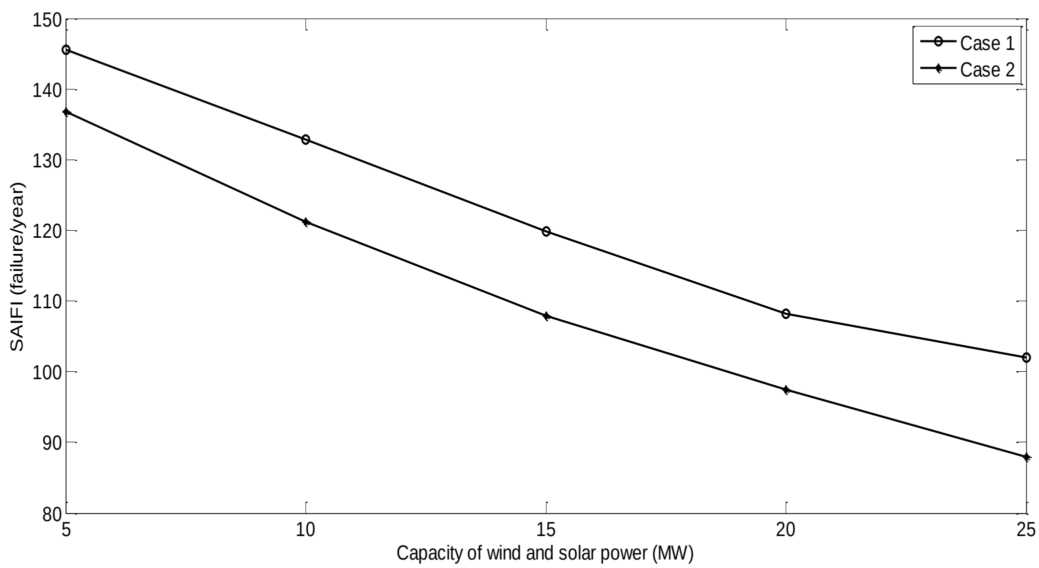

Fig.4.36 Impact of smart restoration on SAIFI

Chapter 5

CONCLUSIONS AND FUTURE RESEARCH

5.1. Conclusions

In this thesis, the impacts of smart restoration, energy storage and wind and solar power capacities have been studied under full wind and solar power penetration in islanded operation. Based on the obtained results from this research, the main conclusions and contributions of this research can be summarized as follow:

- The main contribution of this research is the proposed smart restoration technique for islanded microgrid system which improves the reliability under full penetration of the renewable energy in islanded operation.

- The uncertainty does not affect the system reliability at power capacities compared to the system load but it does at small capacities in terms of SAIDI, SAIFI and EENS.

- The results of the EENS, EENU, down time and failure frequency have shown that increasing of the wind power and solar power reduces the EENS, failure frequency and down time but it increases the EENU largely. Hence, the improvement on the reliability when the wind and solar units are integrated without energy storage is marginal.

- The impact of energy storage on the reliability was positive on SAIDI and SAIFI for both solar and wind energy case studies.

- When the hybrid energy system is considered, the solar power can help in decreasing the EENS at low wind power capacity. Although the low wind and solar power didn’t improve EENS when they were integrated separately.

- The smart restoration has the ability to reduce the EENS, SAIDI and SAIFI at large wind power capacity but it does not able to significantly reduce EENS at small power capacity. On the other hand, Using of the smart restoration will decrease the EENU at all capacities.

- In solar power case, the smart restoration has also the ability to reduce the EENS at large power capacity but it does not able to significantly reduce EENS at small power capacity, while it is able to decrease the EENU at all power capacities. It can’t significantly reduce SAIDI or SAIFI whatever power capacity is.

- In the hybrid case, the smart restoration cannot significantly reduce EENS, SAIDI or SAIFI at small power capacity but it can do at large capacity. While using of the smart restoration in the hybrid case cannot reduce the EENU at all power capacities.

5.2. Future Research

Future research could be focused on the following:

1) Optimizing the location of the dispatchable generator and its power capacity that satisfy certain reliability level.

2) A cost-benefit analysis for integrating dispatchable generator and energy storage system and their optimal capacities.

3) Developing strategy for integrating EV units and their interaction with the renewable energy-based DG.

References

[1] S. Rahman, "Green power: what is it and where can we find it?," *IEEE Power Energy Mag.*, vol. 1, no. 1, pp. 30-37, Jan./Feb. 2003.

[2] C. J. Mozina, "Impact of green power distributed generation," *IEEE Industrial Application Mag.*, vol. 16, no. 4, pp. 55-62, Jul./Aug. 2010.

[3] D. Q. Hung, "Smart Integration of Distributed Renewable Generation and Battery Energy Storage," Thesis for the degree of Doctor of Philosophy, School of Information Technology and Electrical Engineering, The University of Queensland, Australia, 2014.

[4] P. Alberg, "Comparing energy storage options for renewable energy integration," WWEC conference, Cairo, Egypt, 2011.

[5] M. Black and G. Strbac, "Value of bulk energy storage for managing wind power fluctuations," *IEEE Trans. on Energy Conversion.*, vol. 22, no. 1, pp. 197–205, Mar. 2007.

[6] J. P. Barton and D. G. Infield, "Energy storage and its use with intermittent renewable energy," *IEEE Trans. on Energy Conversion.,* vol. 19, no. 2, pp. 441–448, Jun. 2004.

[7] S. D. Jayasinghe, D. Vilathgamuwa, U. K. Madawala, "Direct Integration of Battery Energy Storage Systems in Distributed Power Generation," *IEEE Trans. on energy conversion*, vol. 26, no. 2, Jun/ 2011.

[8] "DG ENER working paper, The future role and challenges of Energy Storage," European Commission, Directorate general for energy, 2012.

[9] A. Kwasinski, V. Krishnamurthy, J. Song, R. Sharma, "Availability Evaluation of Micro-Grids for Resistant Power Supply During Natural Disasters," *IEEE Trans. On Smart Grid,* Vol. 3, no. 4, pp. 2007 – 2018, Dec. 2012.

[10] "What are Smart Micro grids," *Galvin electricity initiative*, http://galvinpower.org/ microgrids, accessed on 6/3/2014.

[11] "The Microgrid Concept," *Micro grid at Berkeley Lab*, http://der.lbl.gov/microgrid -concept, accessed on 6/3/2014.

[12] J. Wentzel, T. Ustun et al., “Investigation of Micro-Grid Behavior While Operating Under Various Network Conditions,” IEEE International Conference on Smart Grid Engineering (SGE’12), Oshawa, Canada 63, 27-29 August, 2012.

[13] C. Xiangyi, L. Bosi et al., “A Reliability Evaluation Method for Distribution System with Microgrids,” 2012 Asia-Pacific Power and Energy Engineering Conference (APPEEC), pp. 1-4, 2012.

[14] “What is reliability of supply?,” EDF energy, https://www.edfenergy.com / energyfuture/ the-energy-gap-reliability-of-supply, 6/3/2014.

[15] “Technology could lead to more reliable renewable energy systems,” Science daily, http://www.sciencedaily.com/releases/2013/12/131203124532.htm, accessed on 2/3/2014.

[16] Y. Luo, L. Wang, G. Zhu, G. Wang “Network Analysis and Algorithm of Microgrid Reliability Assessment,” Asia-Pacific Power and Energy Engineering Conference (APPEEC), 2010.

[17] Q. Chen, L. Mili, “Assessing the Impacts of Microgrids on Composite Power System Reliability,” Power and Energy Society IEEE General Meeting (PES), 2013.

[18] E. Nasrolahpour, M. Doostizadeh et al., “Optimal Management of Micro Grid in Restructured Environment,” 2012 Second Iranian Conference on Renewable Energy and Distributed Generation (ICREDG), Iran, 2012.

[19] W. Haoming, M. Zhengzheng, G. Yong et al., “Analysis of Micro-Grid power supply reliability,” International Conference on Electricity Distribution, China, 2014.

[20] Z. Min-j, L. Ming, “The Study of Distribution Grid Distributed Self-healing under Dynamic Operating Modes,” 2012 China International Conference on Electricity Distribution (CICED 2012), Shanghai, 5-6 Sep. 2012.

[21] Y. Oualmakran, J. Melendez et al., “Self-Healing for Smart Grids: Problem Formulation and Considerations,” 2012 3rd IEEE PES Innovative Smart Grid Technologies Europe (ISGT Europe), Berlin, 2012.

[22] W. Dan , L. Min, "A Survey on Self-healing Control of Smart Distribution Grid," 2012 International Conference on Future Electrical Power and Energy Systems, Lecture Notes in Information Technology, Vol.9, china, 2012.

[23] "Smart distribution: A self-healing and optimized grid," O Power, Electric Light and Power http://www.elp.com/articles/print/volume-91/issue-5/sections/smart-distribution-a-self-healing-and-optimized-grid.html, 6/3/2013.

[24] J. Dong, M. Xiao et al, "Study on technology system of self-healing control in smart distribution grid," IEEE International Conference on Advanced Power System Automation and Protection, China, 2011.

[25] K. Samarakoon, J. Ekanayake, J. Wu, "Smart metering and self-healing of distribution networks," IEEE International Conference on Sustainable Energy Technologies (ICSET), pp. 1-5, 2010.

[26] C. P. Nguyen, A. J. Flueck, "Agent Based Restoration With Distributed Energy Storage Support in Smart Grids," *IEEE Trans. on Smart Grid,* Vol. 3, no. 2, pp. 1029 – 1038, 2012.

[27] Z. Min, Li Ming, "The Study of Distribution Grid Distributed Self-healing under Dynamic Operating Modes," International Conference on Electricity Distribution (CICED), China, 5-6 Sep. 2012.

[28] C. Bo, C. Luwen, W. Zhigang et al., "Study On the Reliability of Integration between Smart Micro-grid and Distribution Network," Power and Energy Engineering Conference (APPEEC), pp. 1-5, 2012.

[29] A. Mohsenzadeh, S. Pazouki, M. Haghifam1, M. E. Talebian, "Impact of DLC Programs Levels on Reliability Improvement of Smart," 8th International Conference on Electrical and Electronics Engineering (ELECO), pp. 72 – 76, 2013.

[30] B. Zhao, X. Dong, J. Bornemann, "Service Restoration for a Renewable-Powered Microgrid in Unscheduled Island Mode," *IEEE Trans. on Smart Grid*, Vol. 6, no. 3, pp. 1128 – 1136, May 2015.

[31] M. Kamh, R. Iravani, T. EL-Fouly, "Realizing a Smart MicroGrid - Pioneer Canadian Experience," Power and Energy Society General Meeting, pp. 1-8, 2012.

[32] Y. Xu, W. Liu, “Novel Multiagent Based Load Restoration Algorithm for Microgrids,” *IEEE Trans. on Smart Grid*, Vol. 2, no. 1, pp. 152 – 161, Mar 2011.

[33] Z. Y. Gao, P. Wang “Reliability Evaluation of Power Systems with WTGs and Energy Storage,” IPEC, Conference Proceedings, pp. 654 – 659, 2010.

[34] W. Y. Li, B. Bagen, “Reliability Evaluation of Integrated Wind/Diesel/Storage Systems for Remote Locations,” IEEE 11th International Conference on Probabilistic Methods Applied to Power Systems (PMAPS), pp. 791 – 795, 2010.

[35] P. Hu, R. Karki, R. Billinton, “Reliability evaluation of generating systems containing wind power and energy storage,” *IET journal and magazine, Generation, Transmission & Distribution,* Vol. 3, no. 8, pp. 783 – 791, 2009.

[36] N. Mendis, K. M. Muttaqi, S. Sayeef et al. “Application of a Hybrid Energy Storage in a Remote Area Power Supply System,” IEEE International Conference on Energy and Exhibition (EnergyCon), pp. 576 – 581, 2010.

[37] I. Krad, E. Ela, V. Koritarov “Quantifying the Operational Benefits of Conventional and Advanced Pumped Storage Hydro on Reliability and Efficiency,” IEEE Conference & Exposition, PES General Meeting, pp. 1-5, 2014.

[38] S. Kahrobaee, S. Asgarpoor, “Reliability-Driven Optimum Standby Electric Storage Allocation for Power Distribution Systems,” 1st IEEE Conference on Technologies for Sustainability (SusTech), pp. 44 - 48, 2013.

[39] C. Gavriluta, I. Candela, J. Rocabert, “Storage system requirements for grid supporting PV-power plants,” IEEE Energy Conversion Congress and Exposition (ECCE), pp. 5323 – 5330, 2014.

[40] R. Karki, H. Po, and R. Billinton, “Reliability evaluation considering wind and hydro power coordination,” *IEEE Trans. Power Syst.*, vol. 25, no. 2, pp. 685–693, 2010.

[41] P. Hu, R. Karki and R. Billinton, “Reliability evaluation of generating systems containing wind power and energy storage”, *IET Generation, Transmission and Distribution*, Vol. 3, no. 8, pp. 783–791, 2009.

[42] P. Bacher, “Short-term Solar Power Forecasting,” Thesis for Master degree in engineering, Informatics and Mathematical Modelling department, Technical University of Denmark, Kongens Lyngby, Denmark, Feb./2008.

[43] V. Margaret, J. Jose, “Exponential Smoothing Models for Prediction of Solar Irradiance,” International Journal of Advanced Research in Electrical on Electronics and Instrumentation Engineering, vol. 4, issue 2, Feb./ 2015.

[44] V. P. Singh, V. Vijay, M. S. Bhatt, D. K. Chaturvedi, “Generalized neural network methodology for short term solar power forecasting,” 13th International Conference on Environment and Electrical Engineering (EEEIC), pp. 58-62, 2013.

[45] Paolik C, Voyant C, Muselli M, Nivet M., “Solar radiation forecasting using ad-hoc time series preprocessing and neural networks,” The 5th international conference on emerging intelligent computing technology and applications, pp. 898-907, Ulsan, South Korea, 2009.

[46] C. Monteiro, T. Santos, L. A. Fernandez-Jimenez, et al., “Short-Term Power Forecasting Model for Photovoltaic Plants Based on Historical Similarity,” *Energies*, vol. 6, pp. 2624-2643, 2013.

[47] Shi, J.; Lee, W.J.; Liu, Y.; Yang, Y.; Wang, P. “Forecasting power output of photovoltaic systems based on weather classification and support vector machines,” *IEEE Trans. on Ind. Appl.* , vol. 48, pp. 1064–1069, 2012.

[48] J. Zeng, W. Qiao, “Short-term solar power prediction using a support vector machine,” *Renewable energy*, vol. 52, pp. 118-127, Apr./ 2013.

[49] P. Krömer, L. Prokop, V. Snasel, S. Misak, et al., “A. Evolutionary Prediction of Photovoltaic Power Plant Energy Production,” In Proceedings of International Conference on Genetic and Evolutionary Computation, pp. 35–42, Philadelphia, PA, USA, 7–11/ Jul./2012.

[50] Y. Wu,C. Chen, H. Abdul Rahman, “A Novel Hybrid Model for Short-Term Forecasting in PV Power Generation,” *Hindawi Publishing Corporation, International Journal of Photoenergy*, vol. 2014, 30 /Jun./ 2014.

[51] Y. Jiang, Z. Song, A. Kusiak, “Very short-term wind speed forecasting with Bayesian structural break model,” *Renewable energy*, vol. 50, pp. 637-647, 2013.

[52] U. Haque, M. Hashem Nehrir, P. Mandal, “A Hybrid Intelligent Model for Deterministic and Quantile Regression Approach for Probabilistic Wind Power Forecasting,” *IEEE Trans. on Power Systems*, vol. 29, issue 4, pp. 1663-1672, 2014.

[53] C. Lei, L. Ran, “Short-Term Wind Speed Forecasting Model for Wind Farm Based on Wavelet Decomposition,” DRPT 2008 , Nanjing, China, 6-9 Apr. / 2008.

[54] N. Chen, Z. Qian, X. Meng, I. T. Nabney, “Short-Term Wind Power Forecasting Using Gaussian Processes,” 23rd international joint conference on artifial intelligence, 2013.

[55] A. Carpinone, R. Langella, A. Testa, M. Giorgio, “Very Short-term Probabilistic Wind Power Forecasting based on Markov Chain Models,” 11th IEEE international conference on probabilistic methods applied to power systems (PMAPS), pp. 107 - 112, 2010.

[56] R. Monteiro, V. Bessa, A. Miranda, A. Botterud, J. Wang and G. Conzelmann, “Wind power forecasting: state-of-the-art 2009,” Argonne National Laboratory; Argonne, Illinois, USA, Tech. Rep. ANL/DIS-10e1, 2009.

[57] L. Ma, S. Luan, C. Jiang, H. Liu, Y. Zhang. “A review on the forecasting of wind speed and generated power,” Renewable and Sustainable Energy Reviews; vol 3:9, 2009.

[58] P. Chen, T. Pedersen, B. Bak-Jensen, Z. Chen, “ARIMA-Based Time Series Model of Stochastic Wind Power Generation,” *IEEE Trans. on Power Systems*, vol 25, no. 2 pp. 667-676, 2010.

[59] A. Andrijanovits, H. Hoimoja, D. Vinnikov, “Comparative Review of Long-Term Energy Storage Technologies for Renewable Energy Systems,” Electronics and Electrical Engineering, no. 2, 2012.

[60] R. Verzijlbergh, L. De Vries, G. Dijkema, P. Herder, “A Note on System Integration to Support a Renewable Energy System,” Faculty of Technology Policy and Management, Delft University of Technology, Jaffalaan 5, 2628BX Delft, The Netherlands, May 27/ 2014.

[61] S. Smith, P. Sen, B. Kroposki, “Advancement of Energy Storage Devices and Applications in Electrical Power System,” IEEE conference, 2008.

[62] K. Nigim, H. Reiser, “Energy Storage for Renewable Energy Combined Heat, Power and Hydrogen Fuel (CHPH 2) Infrastructure,” IEEE Conference on Electrical Power and Energy, 2009.

[63] J. Reddy, D. Reddy, “Probabilistic Performance Assessment of a Roof Top Wind, Solar Photo Voltaic Hybrid Energy System” Annual Symposium on Reliability and Maintainability, pp. 654 – 658, 2004.

[64] D. Parra, G. S. Walker, and M. Gillott, "Modeling of PV generation, battery and hydrogen storage to investigate the benefits of energy storage for single dwelling," Sustainable Cities and Society, vol. 10, pp. 1-10, 2014.

[65] P. Wolfs and G. S. Reddy, "A receding predictive horizon approach to the periodic optimization of community battery energy storage systems," in Universities Power Engineering Conference (AUPEC), 2012 22nd Australasian, pp. 1-6, 2012.

[66] R. Arghandeh and R. Broadwater, "Distributed energy storage control for optimal adoption of solar energy in residential networks," in 2012 20th International Conference on Nuclear Engineering and the ASME 2012 Power Conference, pp. 489-496, 2012.

[67] A. Crossland, D. Jones, and N. Wade, "Planning the location and rating of distributed energy storage in LV networks using a genetic algorithm with simulated annealing," *International Journal of Electrical Power & Energy Systems*, vol. 59, pp. 103-110, 2014.

[68] F. Meng, D. Haughton, B. Chowdhury, M. L. Crow, and G. T. Heydt, "Distributed Generation and Storage Optimal Control With State Estimation," *Smart Grid, IEEE Transactions on,* vol. 4, pp. 2266-2273, 2013.

[69] R. Arghandeh and R. Broadwater, "Distributed energy storage control for optimal adoption of solar energy in residential networks," in 2012 20th International Conference on Nuclear Engineering and the ASME 2012 Power Conference, pp. 489-496, 2012.

[70] “Ottawa (Kanata - Orleans) Historical Wind Speed”, available online at http://ottawa.weatherstats.ca/ download.html, accessed on 1 Apr. /2015.

[71] K. Ogimi, A. Yoza, A. Yona et al., “A Study on Optimum Capacity of Battery Energy Storage System for Wind Farm Operation with Wind Power Forecast Data,” IEEE conference, 2012.

[72] A. Garro, F. Barrara, “Reliability Analysis of Residential Photovoltaic Systems,” International Conference on Renewable Energies and Power Quality, Spain, 13th to 15th April, 2010.

[73] J. Wang; N. Zheng, “A Novel Fractal Image Compression Scheme With Block Classification and Sorting Based on Pearson's Correlation Coefficient,” *IEEE Transactions on Image Processing*, vol. 22, issue 9, pp. 3690-3702, 2013.

[74] K. F. Utsurogi, P. Utsurogi, Giorsetto, “Development of a new procedure for reliability modeling of wind turbine generators,” *IEEE Transactions on Power Apparatus and Systems*, vol. PAS-102, pp. 134-143, Jan/1983.

[75] J. Pinar, F. P. Marquez, A. Tobias, M. Papaelias, “Wind turbine reliability analysis,” *Renewable and Sustainable Energy Reviews*, vol 23, pp. 463-472, Apr./2013.

[76] S. Vittal, M. Teboul, “Performance and Reliability Analysis of Wind Turbines using Monte Carlo Methods based on System Transport Theory,” American Institute for Aeronautics & Astronautics, 2004.

[77] P. J. Tavner, J. Xiang, F. Spinato, “Reliability Analysis for Wind Turbines,” *Wind Energy*, Wiley Interscience, vol. 10, pp. 1-18, 12 Jul./2006.

[78] R. Hill, J. A.Stinebaugh, D. Briand, “Wind Turbine Reliability: A Database and Analysis Approach,” Sandia report 2008, Iussed by Sandia National Laboratories, US Department of Energy, California, USA, Feb. /2008.

[79] Z. Y. Gao, P. Wang, “Reliability Evaluation of Power Systems with WTGs and Energy Storage,” IPEC conference, 2010.

[80] Abouzahr, I. and Ramakumar, R., “An approach to assess the performance of utility-interactive photovoltaic systems,” *IEEE Trans. on Energy Conversion*, v 8, n 2, p 145-53, June 1993.

[81] R. Billinton, R. Karki, “Capacity expansion of small isolated power systems using PV and wind energy,” 2002 IEEE Power Engineering Society Winter Meeting, p 27 vol.1, 2002.

[82] R. Billinton, S. Kumar, N. Chowdhhury, K. Chu, K. Debnath, L. goel, E. Khan, P. Kos, g. Nourbakhsh, and J. Oteng-Adjei, “A Reliability Test System for Educational Purposes-Basic Data,” *IEEE Transactions on Power Systems*, vol.4, pp.1238-1244, 1989.

[83] P. Hu, R. Karki, R. Billinton, “Reliability evaluation of generating systems containing wind power and energy storage,” *IET Generation, Transmission & Distribution*, vol. 3, n 8, p 783-91, August 2009.

[84] M. Korpaas, A. T. Holen, R. Hidrum, “Operation and sizing of energy storage for wind power plants in a market system,” *International Journal of Electrical Power & Energy Systems*, vol. 25, no. 8, pp. 599-606, Oct./ 2003.

[85] A. Gabash and L. Pu, "Active-reactive optimal power flow in distribution networks with embedded generation and battery storage," *IEEE Trans. on Power System.*, vol. 27, no. 4, pp. 2026-2035, Nov./ 2012.

[86] M. Korpas, “Distributed Energy Systems with Wind Power and Energy Storage,” Thesis for the degree of Doctor of Philosophy, Department of Electrical Power Engineering, Norwegian University of Science and Technology, Trondheim, Norway, Mar /2004.

[87] S. X. Chen, H. B. Gooi, and M. Q. Wang, "Sizing of energy storage for microgrids," *IEEE Trans. on Smart Grid*, vol. 3, no. 1, pp. 142-151, Mar./ 2012.

[88] A. Gabash and P. Li, "Flexible optimal operation of battery storage systems for energy supply networks," *IEEE Trans. Power System*, vol. 28, no. 3, pp. 2788-2797, Aug./ 2013.

[89] A. Kamjoo , A. Maheri, G. A. Putrus “Reliability Criteria in Optimal Sizing of Stand-alone Hybrid Wind-PV-Battery bank System,” 2nd International Symposium on Environment Friendly Energies and Applications (EFEA), pp. 184 – 189, 2012.

[90] Z. Y. Gao, P. Wang, “Impacts of Energy Storage on Reliability of Power Systems with WTGs,” PMAPS conference, 2010.

[91] A. Garro, F. Barrara, “Reliability Analysis of Residential Photovoltaic Systems”, International Conference on Renewable Energies and Power Quality (ICREPQ’11), Spain, 13-15 April 2010.

Vitae

Name : Nemer Abd Al Halim Mohammad Amleh

Nationality : Palestinian

Date of Birth : 1/1/1987

Email : nemamleh@yahoo.com

Address : Palestine, Hebron.

Academic Background :

- 2013-2016. MSc. in Electrical engineering, King Fahd University for Petroleum and Minerals (KFUPM)/ Dhahran - KSA.
- 2005-2010 / Bachelor in Electrical Engineering – Polytechnic University /Hebron.

Publications :

1) Amleh Nemer, Al-Awami Ali T., "Optimal Demand Response Bidding and Pricing Mechanism with Fuzzy Optimization: Application for a Virtual Power Plant", Clemson University's power Systems conference 2016, held in Clemson, SC, USA, March 8-11, 2016. [**Won Best Paper Award**]
2) Amleh Nemer, Ata Osama W., "Application of MIMO Smart Antennas into WiMAX-OFDM System in Real Fading IEEE Standardized Channels", Proceedings of the World Congress on Engineering and Computer Science 2012 WCECS 2012, vol. 2, pp. 960-966, San Francisco, USA, October 24-26, 2012.